

## VE-Cadherin–Mediated Epigenetic Regulation of Endothelial Gene Expression

Marco F. Morini,\* Costanza Giampietro,\* Monica Corada, Federica Pisati, Elisa Lavarone, Sara I. Cunha, Lei L. Conze, Nicola O'Reilly, Dhira Joshi, Svend Kjaer, Roger George, Emma Nye, Anqi Ma, Jian Jin, Richard Mitter, Michela Lupia, Ugo Cavallaro, Diego Pasini, Dinis P. Calado, Elisabetta Dejana, Andrea Taddei

**Rationale:** The mechanistic foundation of vascular maturation is still largely unknown. Several human pathologies are characterized by deregulated angiogenesis and unstable blood vessels. Solid tumors, for instance, get their nourishment from newly formed structurally abnormal vessels which present wide and irregular interendothelial junctions. Expression and clustering of the main endothelial-specific adherens junction protein, VEC (vascular endothelial cadherin), upregulate genes with key roles in endothelial differentiation and stability.

**Objective:** We aim at understanding the molecular mechanisms through which VEC triggers the expression of a set of genes involved in endothelial differentiation and vascular stabilization.

**Methods and Results:** We compared a VEC-null cell line with the same line reconstituted with VEC wild-type cDNA. VEC expression and clustering upregulated endothelial-specific genes with key roles in vascular stabilization including *claudin-5*, vascular endothelial-protein tyrosine phosphatase (*VE-PTP*), and von Willebrand factor (*vWf*). Mechanistically, VEC exerts this effect by inhibiting polycomb protein activity on the specific gene promoters. This is achieved by preventing nuclear translocation of FoxO1 (Forkhead box protein O1) and  $\beta$ -catenin, which contribute to PRC2 (polycomb repressive complex-2) binding to promoter regions of *claudin-5*, *VE-PTP*, and *vWf*. VEC/ $\beta$ -catenin complex also sequesters a core subunit of PRC2 (Ezh2 [enhancer of zeste homolog 2]) at the cell membrane, preventing its nuclear translocation. Inhibition of Ezh2/VEC association increases Ezh2 recruitment to *claudin-5*, *VE-PTP*, and *vWf* promoters, causing gene downregulation. RNA sequencing comparison of VEC-null and VEC-positive cells suggested a more general role of VEC in activating endothelial genes and triggering a vascular stability-related gene expression program. In pathological angiogenesis of human ovarian carcinomas, reduced VEC expression paralleled decreased levels of *claudin-5* and *VE-PTP*.

**Conclusions:** These data extend the knowledge of polycomb-mediated regulation of gene expression to endothelial cell differentiation and vessel maturation. The identified mechanism opens novel therapeutic opportunities to modulate endothelial gene expression and induce vascular normalization through pharmacological inhibition of the polycomb-mediated repression system. (*Circ Res.* 2018;122:231-245. DOI: 10.1161/CIRCRESAHA.117.312392.)

**Key Words:** blood vessels ■ cadherin ■ cell differentiation ■ endothelial cells ■ polycomb-group proteins

Several human pathological conditions are characterized by deregulated angiogenesis leading to the formation of unstable blood vessels.<sup>1</sup> Abnormal angiogenesis is also a hallmark of

cancer. Solid tumors get their nourishment from newly formed vessels, which, however, present several structural abnormalities such as wide and irregular interendothelial junctions.<sup>2</sup>

Original received November 14, 2017; revision received November 30, 2017; accepted December 11, 2016. In November 2017, the average time from submission to first decision for all original research papers submitted to *Circulation Research* was 11.99 days.

From the IFOM, FIRC Institute of Molecular Oncology, Milan, Italy (M.F.M., C.G., M.C., F.P., E.D., A.T.); Department of Biomedicine, University of Basel, Switzerland (M.F.M.); Laboratory of Thermodynamics in Emerging Technologies, Department of Mechanical and Process Engineering, ETH Zurich, Switzerland (C.G.); Cogentech, Milan, Italy (F.P.); Department of Experimental Oncology (E.L., D.P.) and Unit of Gynecological Oncology Research (M.L., U.C.), European Institute of Oncology, Milan, Italy; Department of Immunology, Genetics and Pathology, Rudbeck Laboratory, Uppsala University, Sweden (S.I.C., L.L.C., E.D.); Peptide Chemistry (N.O., D.J.), Structural Biology (S.K., R.G.), Experimental Histopathology (E.N.), Bioinformatics & Biostatistics Department (R.M.), and Immunity and Cancer Laboratory (D.P.C., A.T.), The Francis Crick Institute, London, United Kingdom; Center for Chemical Biology and Drug Discovery, Departments of Pharmacological Sciences and Oncological Sciences, Tisch Cancer Institute, Icahn School of Medicine at Mount Sinai, New York, NY (A.M., J.J.); and Department of Oncology and Hemato-Oncology, University of Milan, Italy (E.D.).

\*M.F. Morini and C. Giampietro contributed equally to this study.

The online-only Data Supplement is available with this article at <http://circres.ahajournals.org/lookup/suppl/doi:10.1161/CIRCRESAHA.117.312392/-/DC1>.

Correspondence to Andrea Taddei, PhD, Immunity and Cancer Laboratory, The Francis Crick Institute, 1 Midland Rd, London NW1 1AT, United Kingdom, E-mail [andrea.taddei@crick.ac.uk](mailto:andrea.taddei@crick.ac.uk); or Elisabetta Dejana, Prof, PhD, IFOM, FIRC Institute of Molecular Oncology, Via Adamello 16, 20139 Milan, Italy, E-mail [elisabetta.dejana@ifom.eu](mailto:elisabetta.dejana@ifom.eu)

© 2017 The Authors. *Circulation Research* is published on behalf of the American Heart Association, Inc., by Wolters Kluwer Health, Inc. This is an open access article under the terms of the [Creative Commons Attribution](https://creativecommons.org/licenses/by/4.0/) License, which permits use, distribution, and reproduction in any medium, provided that the original work is properly cited.

*Circulation Research* is available at <http://circres.ahajournals.org>

DOI: 10.1161/CIRCRESAHA.117.312392

## Novelty and Significance

### What Is Known?

- Pathological conditions such as inflammation, diabetic retinopathy, and age-related macular degeneration are characterized by deregulated angiogenesis and unstable blood vessels.
- Solid tumors receive nutrients and oxygen from newly formed vessels that display structural abnormalities such as lack of hierarchy, abnormal lumen, altered endothelial cell–cell junctions, and poor control of permeability.
- VEC (vascular endothelial cadherin) and its clustering at cell–cell adherens junctions upregulate claudin-5, key component of endothelial tight junctions regulating vessel permeability, via inhibition of FoxO1 (Forkhead box protein O1) and  $\beta$ -catenin nuclear translocation.

### What New Information Does This Article Contribute?

- VEC expression and clustering upregulate a wide set of genes involved in endothelial differentiation and vascular stabilization, such as vascular endothelial-protein tyrosine phosphatase (*VE-PTP*) and von Willebrand factor (*vWF*) along with previously identified *claudin-5*.
- *Claudin-5*, *VE-PTP*, and *vWF* are expressed via inhibition of polycomb protein binding to their promoters by preventing the nuclear accumulation of FoxO1 and  $\beta$ -catenin, which associate with PRC2 (polycomb repressive complex-2) and promote its localization at target genes.
- VEC sequesters Ezh2 (enhancer of zeste homolog 2), a key component of PRC2, at the plasma membrane in a  $\beta$ -catenin–dependent and p120-catenin–dependent manner, further reducing polycomb nuclear activity.

Solid tumors and other human pathologies display abnormal, destabilized blood vessels, with wide and irregular endothelial cell–cell junctions. These leaky vessels favor metastatic dissemination of tumor cells, cause hemorrhages, and reduce delivery of therapeutic agents. We found that VEC is able to coordinate the expression of genes involved in endothelial differentiation and vascular stabilization. In particular, VEC expression and clustering upregulate stability-related genes *claudin-5*, *VE-PTP*, and *vWF* by preventing polycomb protein binding to their promoters via inhibition of FoxO1/ $\beta$ -catenin nuclear localization and sequestration of PRC2 component Ezh2 at the plasma membrane. This study shows that adherens junction establishment influences chromatin organization by modulating polycomb activity and that cadherin-mediated recruitment of a polycomb protein can influence gene expression. This mechanism depends on cadherin type, as no Ezh2/N-cadherin interaction is observed. Moreover, the work highlights a new role for FoxO1/ $\beta$ -catenin complex in localizing polycombs at target endothelial gene promoters. In vessels of human ovarian carcinomas, downregulation of VEC parallels reduced *Claudin-5* and *VE-PTP* expression, pointing at a possible involvement of the identified mechanism. The data presented here suggest therapeutic opportunities to induce vascular normalization through inhibition of the polycomb-mediated repression system in pathological states characterized by vascular leakiness and fragility.

### Nonstandard Abbreviations and Acronyms

|                 |  |
|-----------------|--|
| <b>Adm</b>      | adrenomedullin   |
| <b>AJs</b>      | adherens junctions   |
| <b>Ang</b>      | angiopoietin   |
| <b>ECs</b>      | endothelial cells  |
| <b>Eed</b>      | embryonic ectoderm development                                 |
| <b>Ezh2</b>     | enhancer of zeste homolog 2                                    |
| <b>H3K27me3</b> | histone H3 trimethylated on lysine 27                          |
| <b>Hey1</b>     | Hes-related family bHLH transcription factor with YRPW motif-1 |
| <b>HMEC-1</b>   | human dermal microvascular endothelial cells-1                 |
| <b>IL</b>       | interleukin  |
| <b>Lmo2</b>     | LIM domain only-2  |
| <b>PcG</b>      | polycomb group   |
| <b>Pecam1</b>   | platelet/endothelial cell adhesion molecule-1                  |
| <b>PI3K</b>     | phosphatidylinositol 3 kinase                                  |
| <b>PRC</b>      | polycomb repressive complex                                    |
| <b>Rbap48</b>   | retinoblastoma-binding protein 48                              |
| <b>Sox18</b>    | SRY (sex determining region Y)-box-18                          |
| <b>Stat6</b>    | signal transducer and activator of transcription-6             |
| <b>Suz12</b>    | suppressor of zeste 12   |
| <b>TAT</b>      | transactivator of transcription                                |
| <b>Tcf</b>      | T-cell factor  |
| <b>TCF4-DN</b>  | dominant negative form of Tcf4                                 |
| <b>Tiam1</b>    | T-cell lymphoma invasion and metastasis-1                      |
| <b>TJ</b>       | tight junction   |
| <b>TrxG</b>     | trithorax group  |

### Nonstandard Abbreviations and Acronyms Continued

|               |   |
|---------------|---|
| <b>TSS</b>    | transcription start site                          |
| <b>VEC</b>    | vascular endothelial cadherin                     |
| <b>VEGFR2</b> | vascular endothelial growth factor receptor-2     |
| <b>VE-PTP</b> | vascular endothelial-protein tyrosine phosphatase |
| <b>vWf</b>    | von Willebrand factor                             |

VEC (vascular endothelial cadherin), the main component of endothelial adherens junctions (AJs), plays a major role in the process of vessel maturation and stability. This molecule, specifically expressed by endothelial cells (ECs), mediates homophilic adhesion at cell–cell contacts regulating vascular permeability.<sup>3</sup> VEC is indispensable for vascular maturation and inhibition of vascular regression.<sup>3</sup> VEC clustering at AJs triggers intracellular signals inducing contact inhibition of cell growth, protection from apoptosis, cell polarity, and inhibition of migration.<sup>4</sup>

In previous work, we found that VEC expression and clustering at cell–cell contacts relieve the inhibitory effect of the FoxO1 (Forkhead box protein O1)/ $\beta$ -catenin complex on the expression of *claudin-5*, an endothelial-specific TJ (tight junction) protein,<sup>5</sup> acting via the removal of a transcriptional repression mechanism.

The reversible nature of *claudin-5* gene repression suggested the involvement of PcG (polycomb group) proteins and epigenetic mechanisms in VEC-mediated regulation of *claudin-5* expression. Indeed, PcG proteins control the induction of reversible states of epigenetic silencing in most

(Continued)

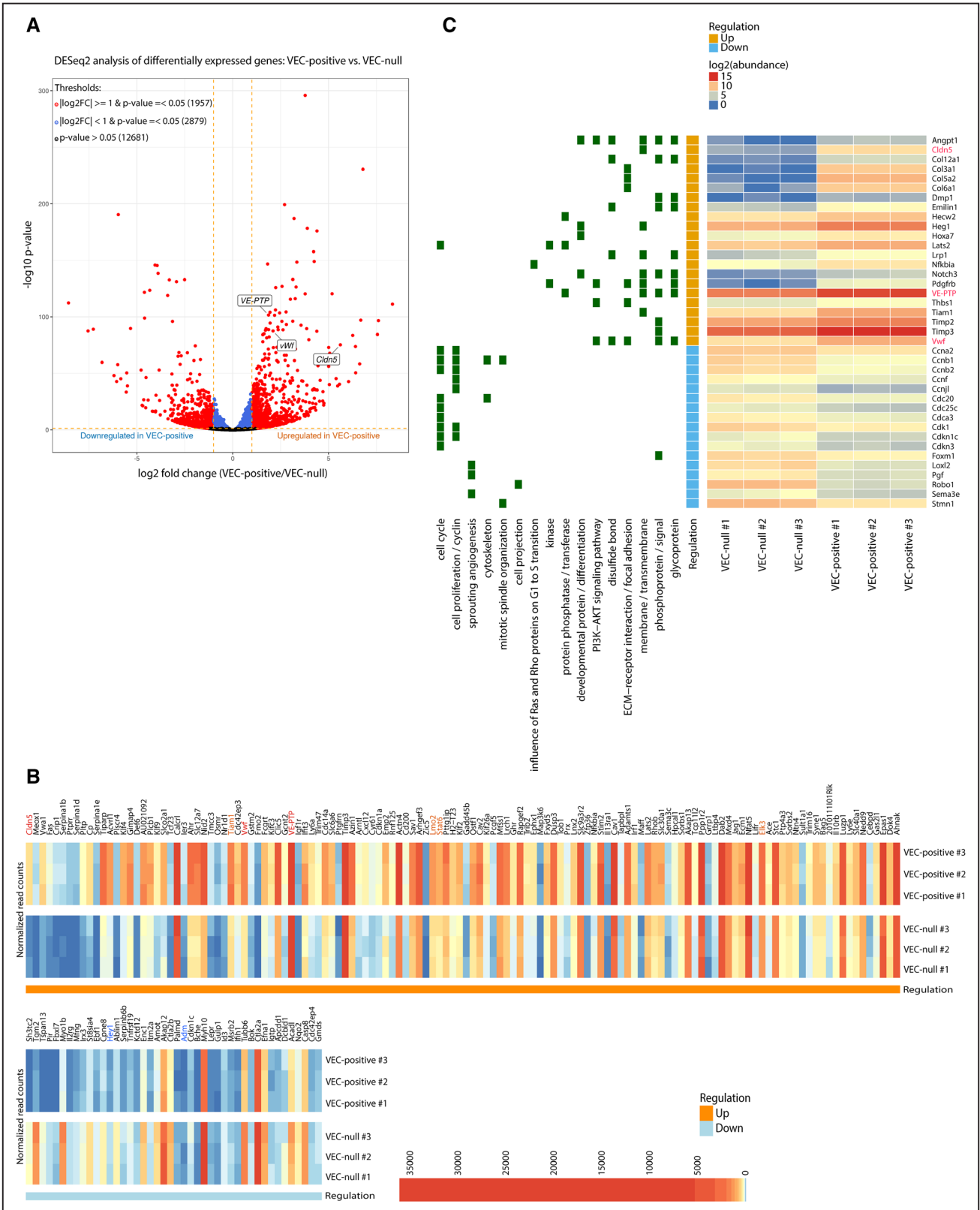


**Figure 1. Transcriptome profile determined by VEC (vascular endothelial cadherin) expression and clustering. A,** Volcano plot showing the magnitude of differential expression between VEC-positive and VEC-null endothelial cells (ECs). Each dot represents 1 gene with detectable expression in both cell types. The horizontal dashed line (orange) together with the vertical lines (orange) mark thresholds used ( $P$  value  $\leq 0.05$  and  $|\log_2FC| \geq 1$ ) to define a gene as differentially regulated in VEC-positive (red). Genes that only passed threshold  $P$  value  $\leq 0.05$  are depicted in blue. Dots representing *claudin-5*, vascular endothelial-protein tyrosine phosphatase (*VE-PTP*), and von Willebrand factor (*vWF*) are labeled in the figure. **B,** Heat-map showing the expression pattern of significantly differentially expressed endothelial genes ( $P$  value  $\leq 0.05$  and  $|\log_2FC| \geq 1$ ) within and between biological replicates. Endothelial genes upregulated (red/orange) or downregulated (blue) in VEC-positive cells which were further investigated in this study are highlighted in the figure. Genes (*Continued*)

multicellular organisms, including humans, and regulate several developmental decisions by silencing genes involved in stem cell differentiation and specification of cellular identities.<sup>6,7</sup> Their activity is exerted through 2 multiprotein complexes called PRC (polycomb repressive complex)1 and PRC2.<sup>6</sup> PRC2 core subunits are Ezh (enhancer of zeste homolog)2, Suz (suppressor of zeste)12, Eed (embryonic ectoderm development), and Rbap (retinoblastoma-binding protein)48. Ezh2 is the catalytic subunit containing a SET [Su(var)3-9, enhancer of zeste and trithorax] domain, which harbors the active site for histone H3 trimethylation on lysine 27, although Suz12 and Eed association is needed for optimal enzymatic activity.<sup>8</sup> According to the canonical model, H3K27me3 (histone H3 trimethylated on lysine 27) is a silencing histone mark promoting the recruitment of PRC1 selectively at genes that are targeted for repression. PRC1 includes Ring1B, which mediates monoubiquitylation of histone H2A on lysine 119<sup>9</sup> blocking gene expression by multiple mechanisms such as chromatin compaction, inhibition of transcriptional initiation or elongation, recruitment of transcriptional inhibitors, and block of the binding of key activators.<sup>6,10</sup>

A fundamental step in PRC-mediated transcriptional repression is the ability of such complexes to be recruited specifically at target genes. In *Drosophila*, this is accomplished by polycomb response elements, clusters of DNA-binding sites for proteins that associate with PRC2 and PRC1.<sup>11</sup> Mammalian polycomb response elements have not been identified yet, and many aspects of polycomb recruitment still remain obscure.

Here, we report that VEC-mediated inhibition of FoxO1/β-catenin nuclear accumulation triggers a transcriptional program of endothelial differentiation and maturation. PcG proteins exert an essential role in such program by targeting the promoters of key endothelial stability genes *claudin-5*, vascular endothelial-protein tyrosine phosphatase (*VE-PTP*), and von Willebrand factor (*vWf*), causing their repression. VEC can inhibit such mechanism in multiple ways, by preventing polycomb binding to gene promoters through restriction of the nuclear localization of the FoxO1/β-catenin complex and by sequestering a fraction of Ezh2 at the plasma membrane.

These observations are supported by *in vivo* data in newborn mice treated with Ezh2 inhibitor UNC1999. Furthermore, dismantling of VEC clusters during pathological angiogenesis in human ovarian carcinomas is accompanied by the downregulation of Claudin-5 and VE-PTP.

These data highlight a key role of PcG proteins in the regulation of EC gene expression and open novel therapeutic opportunities to induce vascular normalization through pharmacological inhibition of the polycomb-mediated repression system.

## Methods

Detailed Methods section is available in the [Online Data Supplement](#).

The data that support the findings of this study are available from the corresponding author on reasonable request.

## Results

### VEC Clustering Triggers an Endothelial-Specific Transcription Program

To investigate whether VEC was able to upregulate other endothelial-specific genes besides *claudin-5*,<sup>5</sup> we performed an RNA sequencing comparative analysis of a mouse VEC-null cell line (VEC-null) and the same line reconstituted with VEC wild-type cDNA (VEC-positive). Several genes were upregulated by VEC expression and clustering (Figure 1A). Taking advantage of previously published data on endothelial gene expression,<sup>12</sup> we selected a list of endothelial genes whose expression was induced or repressed by VEC (Figure 1B; Online Tables I and II). Further validation of RNA sequencing data was performed by quantitative real-time polymerase chain reaction of *VE-PTP*,<sup>13</sup> *vWf*,<sup>14</sup> T-cell lymphoma invasion and metastasis-1 (*Tiam1*),<sup>15</sup> LIM domain only-2 (*Lmo2*),<sup>16</sup> signal transducer and activator of transcription-6 (*Stat6*)<sup>17</sup> and *Elk3* (ETS domain containing protein)<sup>18,19</sup> among VEC-induced genes, hes-related family bHLH transcription factor with YRPW motif-1 (*Hey1*)<sup>20</sup> and adrenomedullin (*Adm*)<sup>21</sup> among VEC-repressed genes, and platelet/endothelial cell adhesion molecule-1 (*Pecam1*)<sup>22</sup> and SRY (sex determining region Y)-box-18 (*Sox18*)<sup>19</sup> as genes not influenced by VEC expression (Online Figures IA and IIA through IIC). Similar transcriptional changes were induced by VEC clustering when comparing human dermal microvascular ECs (HMEC-1) in sparse and confluent conditions (Online Figure IID through IIG). Interestingly, VEC also seemed to coordinate the expression of several genes promoting vascular stability, according DAVID Functional Annotation Clustering tool.<sup>23</sup> For instance, we observed a general downregulation of genes involved in cell proliferation and sprouting angiogenesis, while extracellular matrix interaction and cell–cell adhesion were promoted (Figure 1C).

Within VEC-upregulated endothelial genes, we selected the tyrosine phosphatase *VE-PTP*<sup>13</sup> and the extracellular matrix protein *vWf*<sup>14</sup> for further studies. These 2 genes were selected by virtue of their endothelial specificity and their described role in the induction of vascular stability.<sup>13,14</sup> As reported for *claudin-5*,<sup>5</sup> both genes were strongly upregulated by VEC expression and clustering (Online Figure IA). A mutant version of VEC composed of the cadherin cytoplasmic tail fused to the transmembrane and extracellular domains of IL-2 (interleukin-2) receptor α-chain (IL2-VEC),<sup>5</sup> which is unable to cluster at cell–cell contacts, did not upregulate these genes, confirming the need of VEC clustering for this effect (Online Figure III). As for *claudin-5*,<sup>5</sup> FoxO1 and β-catenin activity inhibited *VE-PTP* and *vWf* expression. Infection of confluent VEC-positive cells with an adenovirus encoding a constitutively active form of FoxO1 (FKHR-TM [Forkhead transcription factor triple mutant])<sup>24</sup> significantly downregulated both *VE-PTP* and *vWf* expression (Online Figure IB). Similarly, increasing endogenous FoxO1 activity by LY294002-mediated inhibition of PI3K (phosphatidylinositol 3 kinase) reduced FoxO1-Ser256 (serine 256) phosphorylation

**Figure 1 Continued.** are displayed in decreasing  $|\log_2FC|$  order (left to right). **C**, Heat-map showing normalized abundance of significantly changing genes across all samples. Genes belonging to selected functionally enriched terms are highlighted in green on the left of the plot. *Claudin-5*, *VE-PTP*, and *vWf* genes are highlighted in red. In **(B)** and **(C)**, VEC-positive numbers 1/2/3 represent biological replicates in VEC-positive cells, whereas VEC-null numbers 1/2/3 represent biological replicates in VEC-null cells.

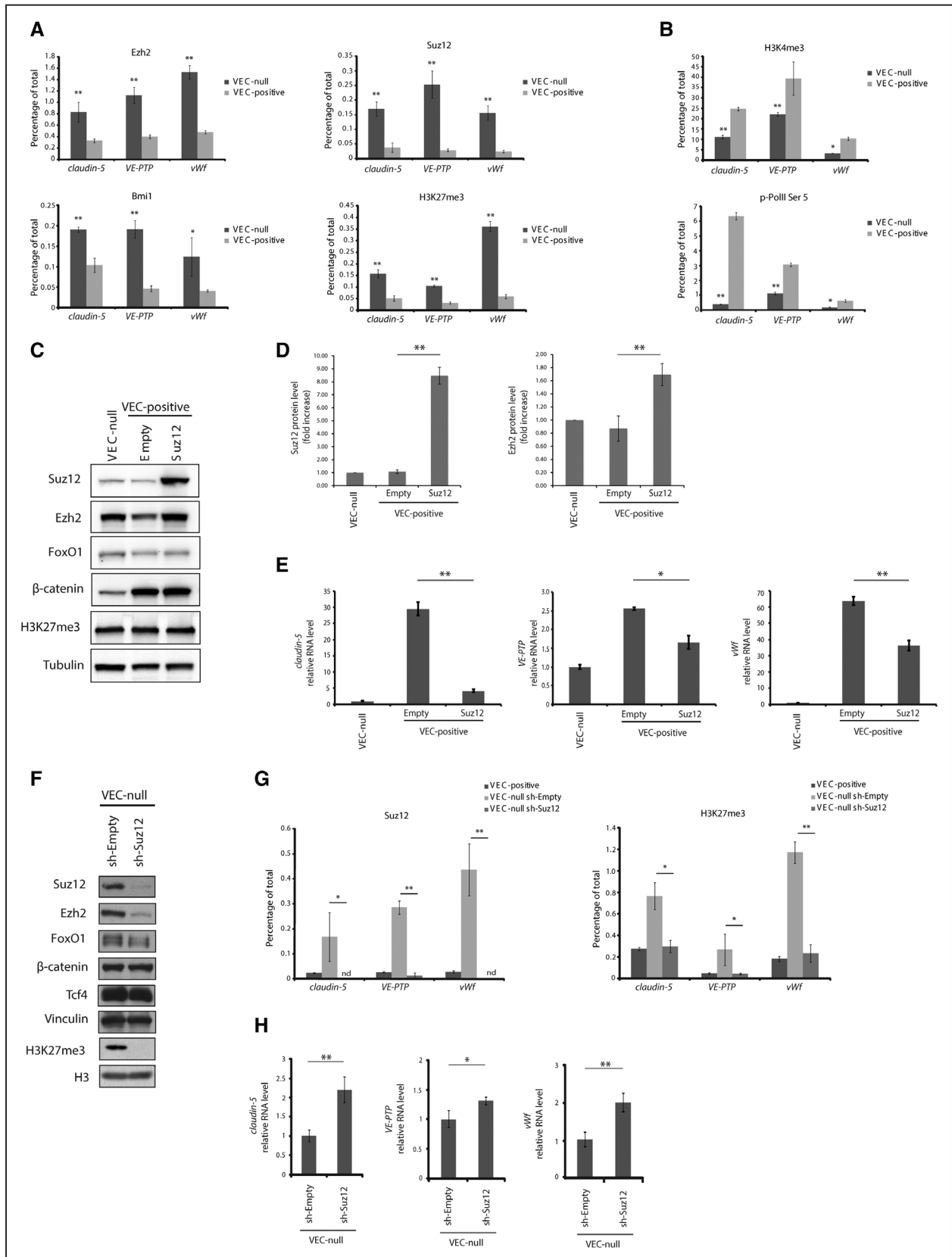


**Figure 2. *Claudin-5*, vascular endothelial-protein tyrosine phosphatase (*VE-PTP*), and von Willebrand factor (*vWf*) are polycomb targets.** **A**, Quantitative real-time polymerase chain reaction (qRT-PCR) for the transcription start site (TSS) of *claudin-5*, *VE-PTP*, and *vWf* performed on endogenous *Ezh2* (enhancer of zeste homolog 2)-, *Suz12* (suppressor of zeste 12)-, *Bmi1* (B lymphoma Mo-MLV insertion region 1)-, and H3K27me3 (histone H3 trimethylated on lysine 27)-bound chromatin immunoprecipitated from confluent VEC (vascular endothelial cadherin)-null and VEC-positive endothelial cells (ECs). **B**, qRT-PCR for the TSS of *claudin-5*, *VE-PTP*, and *vWf* (Continued)

level (Online Figure IC, upper) and downregulated both genes under study (Online Figure IC).  $\beta$ -Catenin associates with FoxO1 and stabilizes its binding to *claudin-5* promoter.<sup>5</sup> The expression of a stabilized version of  $\beta$ -catenin ( $\Delta N$ - $\beta$ -catenin)<sup>5</sup> led to a marked downregulation of both *VE-PTP* and *vWf* genes (Online Figure ID), suggesting a regulatory mechanism similar to that of *claudin-5*. A promoter analysis spanning from 6000 bp upstream to 500 bp downstream of the transcription start site (TSS) of *VE-PTP* and *vWf* genes identified a series of paired Tcf (T-cell factor)/ $\beta$ -catenin/FoxO1-binding sites localized in 3 different regions on both promoters (Online Figure IE). Quantitative chromatin immunoprecipitation showed that FoxO1 binds all 3 regions in both promoters (Online Figure IF). Binding occurred only in confluent VEC-null and not in confluent VEC-positive cells, correlating with gene repression. Furthermore,  $\beta$ -catenin also bound all identified regions with different affinity (Online Figure IG), consistently with what previously reported.<sup>5</sup> Thus, VEC upregulates the endothelial-specific genes *vWf* and *VE-PTP* through a mechanism similar to *claudin-5* upregulation.

### **Claudin-5, VE-PTP, and vWf Are Polycomb Target Genes**

We then aimed at clarifying how the FoxO1/ $\beta$ -catenin complex might act on *claudin-5*, *VE-PTP*, and *vWf* genes to induce their repression. Given the endothelial specificity of the identified genes, we hypothesized the possible involvement of PcG proteins, a group of transcriptional regulators involved in cell specification, which mediate reversible inhibition of transcription.<sup>6</sup> We performed quantitative chromatin immunoprecipitation for PcG proteins on the TSS of *claudin-5*, *VE-PTP*, and *vWf* genes. Gene TSSs displayed higher enrichment in the components of both PRC2 (Ezh2 and Suz12) and PRC1 (Bmi1; B lymphoma Mo-MLV insertion region 1) in confluent VEC-null compared with VEC-positive cells (Figure 2A, top and lower left). The mark of Ezh2 enzymatic activity, H3K27me3, also showed a similar enrichment pattern (Figure 2A, lower right), and quantitative chromatin immunoprecipitation for total histone H3 showed comparable enrichments at the analyzed regions in VEC-null and VEC-positive cells (Online Figure IV), ruling out the possibility that the higher H3K27me3 signal in VEC-null cells could be because of widespread higher histone density. PcG-mediated repression is counteracted by the activity of TrxG (trithorax group) proteins.<sup>6</sup> As expected, *claudin-5*, *VE-PTP*, and *vWf* TSSs showed a higher enrichment in H3K4me3, marker of TrxG activity and gene activation, in confluent VEC-positive cells than in VEC-null cells (Figure 2B, upper). RNA polymerase II phosphorylated on Ser5, a modification needed for the enzyme to escape the promoter and transcribe the gene,

was also increased at the TSSs of genes in confluent VEC-positive cells (Figure 2B, lower).

When we overexpressed the PRC2 member Suz12 in confluent VEC-positive cells using lentiviral-mediated gene delivery (Figure 2C), *claudin-5*, *VE-PTP*, and *vWf* expression was reduced (Figure 2E). PRC2 proteins are known to promote each other's stability by physical interaction.<sup>8</sup> Suz12 overexpression led to an almost 2-fold increase in Ezh2 protein level (Figure 2D). The promoter region of *claudin-5* (3169 bp upstream of the coding sequence; Online Figure VA), comprising all 3 regions of paired Tcf/ $\beta$ -catenin/FoxO1-binding sites<sup>5</sup> was cloned upstream of the firefly luciferase gene. As expected, transfection of this reporter in confluent VEC-null and VEC-positive cells showed higher luciferase activity in the presence of VEC expression and clustering (Online Figure VB). Suz12 overexpression in VEC-positive ECs significantly decreased luciferase expression (Online Figure VC). *Lmo2* and *Stat6* were also downregulated by Suz12 overexpression (Online Figure VIA), suggesting that the identified mechanism might regulate a wider set of endothelial genes. *Hey1* expression was induced by Suz12 (Online Figure VIB), likely as a result of polycomb-mediated downregulation of a *Hey1* gene repressor, while *Pecam1* and *Sox18* levels were not altered (Online Figure VIC). Conversely, Suz12 knockdown led to a marked decrease in Ezh2 and to the abrogation of detectable H3K27me3 levels (Figure 2F). FoxO1 protein levels were  $\approx 30\%$  lower on Suz12 knockdown (Figure 2F), although FoxO1 mRNA expression was unchanged (Online Figure VII). Suz12 knockdown abolished Suz12 and H3K27me3 signal at the TSSs of *claudin-5*, *VE-PTP*, and *vWf* genes (Figure 2G) causing a partial reactivation of their expression (Figure 2H). The incomplete rescue of expression might be because of the lack of specific gene activators missing in a VEC-null context or to PRC1 activity keeping genes partially repressed in the absence of PRC2.<sup>25</sup> Furthermore, Suz12 knockdown induced an increase in *claudin-5* promoter activity as assessed by luciferase reporter assay (Online Figure VD).

### **FoxO1/ $\beta$ -Catenin Enhance PcG Protein Binding to *Claudin-5*, *VE-PTP*, and *vWf* Promoters**

We then hypothesized that the FoxO1/ $\beta$ -catenin complex could positively modulate polycomb interaction with the promoters of the identified genes. By coimmunoprecipitation, we found that constitutively active FKHR-TM or endogenous FoxO1 interact with Ezh2 (Figure 3A). Another member of PRC2, Suz12, also coimmunoprecipitated with FKHR-TM (Figure 3B). FKHR-TM overexpression in VEC-positive confluent cells increased PcG protein binding to the

**Figure 2 Continued.** performed on endogenous H3K4me3-bound and RNA polymerase II (p-PolII) Ser5-bound chromatin immunoprecipitated from confluent VEC-null and VEC-positive ECs. **C**, Western blot (WB) analysis of indicated proteins in extracts of confluent VEC-null and VEC-positive ECs upon Suz12 overexpression. **D**, Quantification of WB in **(C)**. Suz12 and Ezh2 levels were normalized to tubulin. Columns are means $\pm$ SEM of 3 independent experiments. **E**, qRT-PCR analysis of *claudin-5*, *VE-PTP*, and *vWf* expression in confluent VEC-null and VEC-positive ECs upon Suz12 overexpression. **F**, WB analysis of indicated proteins in extracts of confluent VEC-null ECs upon Suz12 knockdown (sh-Suz12). **G**, qRT-PCR for the TSS of *claudin-5*, *VE-PTP*, and *vWf* performed on endogenous Suz12- and H3K27me3-bound chromatin immunoprecipitated from confluent VEC-positive, VEC-null-sh-Empty, and VEC-null-sh-Suz12 ECs. **H**, qRT-PCR analysis of *claudin-5*, *VE-PTP*, and *vWf* expression in confluent VEC-null-sh-Empty and VEC-null-sh-Suz12 ECs. **A**, **B**, **G**, Levels of DNA are normalized to input, columns are means $\pm$ SD of triplicates from a representative experiment. **C**, **F**, Tubulin and vinculin are the loading controls. **E**, **H**, Levels of mRNA are normalized to 18S; columns are means $\pm$ SEM of triplicates from a representative experiment. In **(A)** and **(B)**, \* $P < 0.05$ ; \*\* $P < 0.01$ , *t* test VEC-null vs VEC-positive. In **(G)**, \* $P < 0.05$ ; \*\* $P < 0.01$ , *t* test VEC-null Sh-Empty vs VEC-null Sh-Suz12. In **(D)**, **(E)**, and **(H)**, \* $P < 0.05$ ; \*\* $P < 0.01$ , *t* test. nd indicates not detectable.

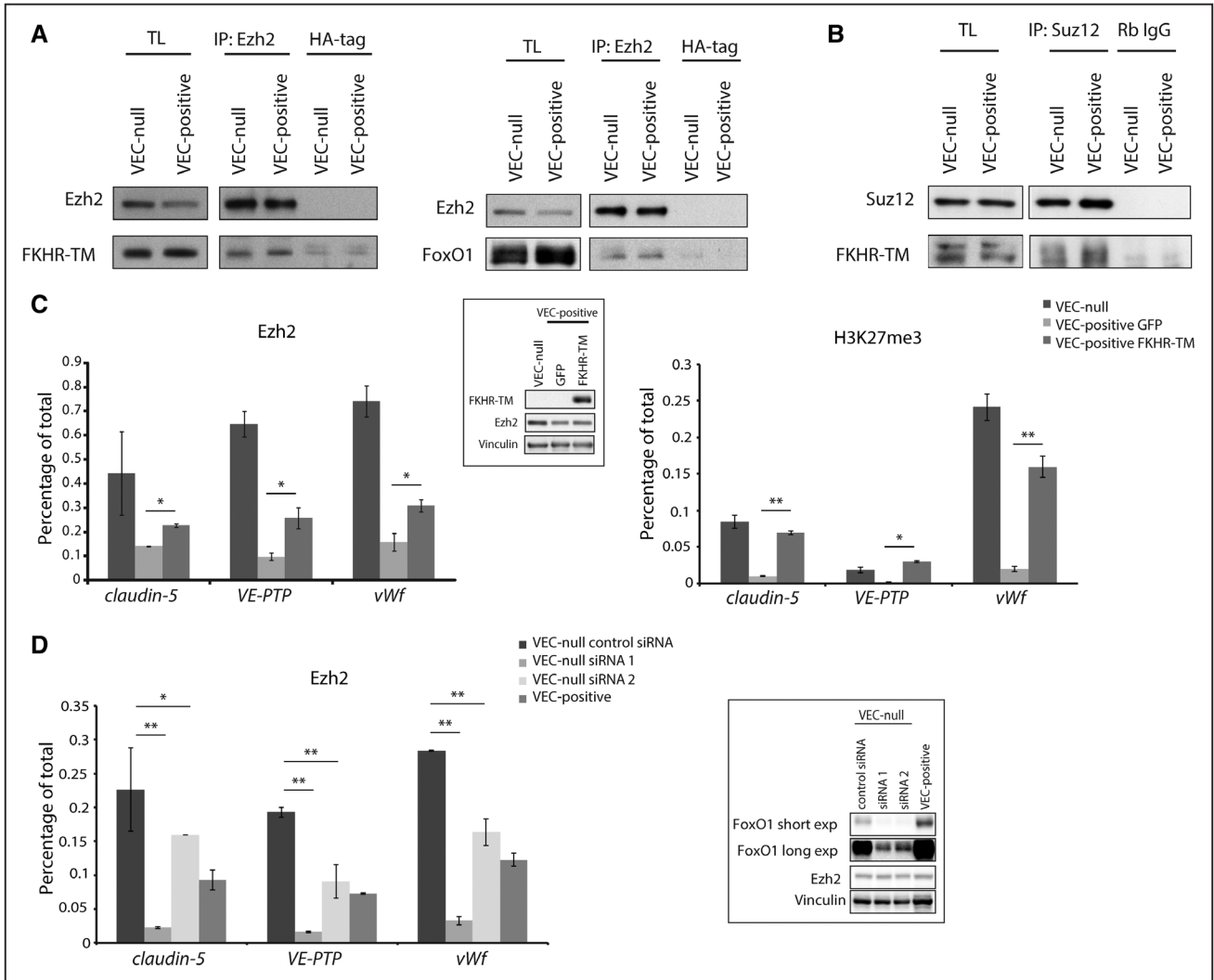


**Figure 3.** FoxO1 (Forkhead box protein O1) enhances PcG (polycomb group) protein association to *claudin-5*, vascular endothelial-protein tyrosine phosphatase (*VE-PTP*), and von Willebrand factor (*vWf*) promoters. **A, B**, Coimmunoprecipitation and Western blot (WB) of endogenous Ezh (enhancer of zeste homolog)2 or Suz (suppressor of zeste)12 and endogenous FoxO1 or FKHR-TM (Forkhead transcription factor triple mutant) from extracts of confluent VEC (vascular endothelial cadherin)-null and VEC-positive endothelial cells (ECs) or the same cells types expressing FKHR-TM (myc-tagged). **C**, Quantitative real-time polymerase chain reaction (qRT-PCR) for the transcription start site (TSS) of *claudin-5*, *VE-PTP*, and *vWf* performed on endogenous Ezh2- and H3K27me3 (histone H3 trimethylated on lysine 27)-bound chromatin immunoprecipitated from confluent VEC-null and VEC-positive ECs expressing either FKHR-TM or GFP (green fluorescent protein; negative control). Inset: WB analysis of FKHR-TM and Ezh2. **D**, qRT-PCR for the TSS of *claudin-5*, *VE-PTP*, and *vWf* performed on endogenous Ezh2-bound chromatin immunoprecipitated from confluent VEC-positive or VEC-null ECs transfected with control siRNA or with 2 siRNAs targeting FoxO1 mRNA. Inset: WB analysis of FoxO1 and Ezh2. Two different film exposure timings are shown for FoxO1. **C, D**, Vinculin is the loading control. Levels of DNA are normalized to input, columns are means $\pm$ SD of triplicates from a representative experiment. In **(C)**, \* $P$ <0.05; \*\* $P$ <0.01,  $t$  test VEC-positive GFP vs VEC-positive FKHR-TM. In **(D)**, \* $P$ <0.05; \*\* $P$ <0.01,  $t$  test VEC-null control siRNA vs VEC-null siRNA1 or VEC-null siRNA2. IP indicates immunoprecipitation; and TL, total cell lysate.

TSS of *claudin-5*, *VE-PTP*, and *vWf* genes, as shown by Ezh2 quantitative chromatin immunoprecipitation (Figure 3C, left). Consequently, H3K27me3 repressive histone mark was increased (Figure 3C, right). This is consistent with gene downregulation observed on FKHR-TM overexpression (Online Figure IB). No increase in Ezh2 protein levels was induced by FKHR-TM (Figure 3C inset), proving that the augmented Ezh2 enrichment was independent of protein up-regulation. Conversely, FoxO1 knockdown strongly reduced Ezh2 recruitment at target sites in VEC-null cells to levels comparable to those detected in VEC-positive cells, or even lower (Figure 3D), in the absence of any Ezh2 downregulation

(Figure 3D inset). Interestingly, this effect was dose dependent. SiRNA 2 was less efficient than siRNA 1 in knocking down FoxO1 (see FoxO1 long exp, Figure 3D inset), and this resulted in a weaker reduction of Ezh2 binding to gene TSSs.

Coexpression of Suz12 and FKHR-TM in VEC-positive confluent cells induced a stronger repression of *claudin-5* than the expression of FKHR-TM alone (75.3% versus 53.1%; Online Figure VIIIA and VIIIB), further supporting the hypothesis that FoxO1 acts in concert with polycomb activity.

We then investigated whether  $\beta$ -catenin could interact with PcG protein complex. Coimmunoprecipitation experiments showed an interaction between  $\beta$ -catenin and both Ezh2

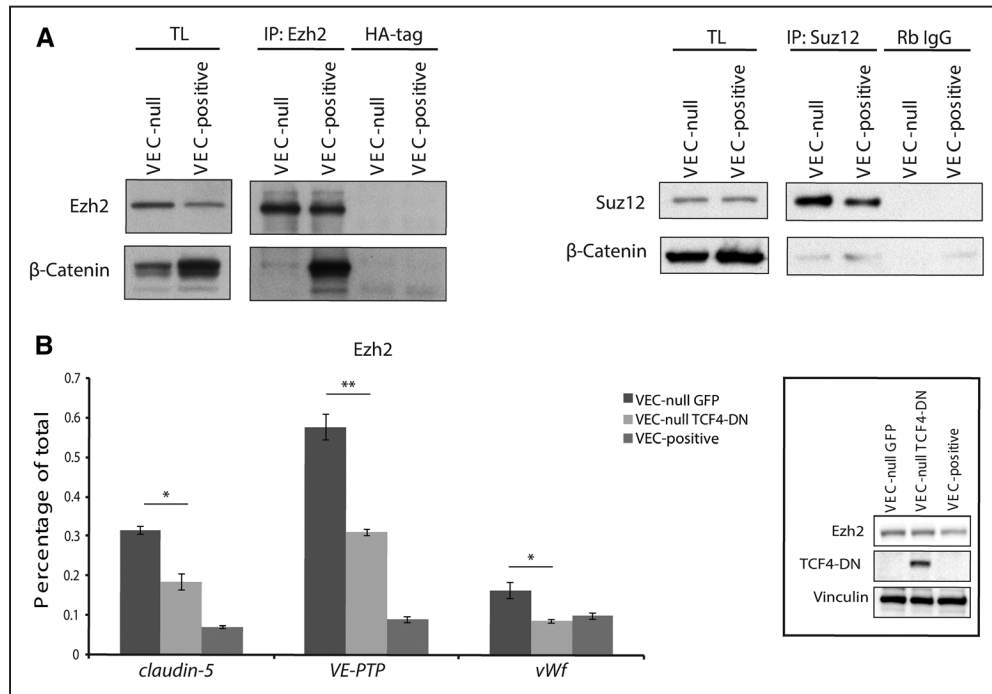


**Figure 4.**  $\beta$ -Catenin stabilizes polycomb/DNA interaction on *claudin-5*, vascular endothelial-protein tyrosine phosphatase (*VE-PTP*), and von Willebrand factor (*vWf*) promoters. **A**, Coimmunoprecipitation and Western blot (WB) analysis of endogenous Ezh2 (enhancer of zeste homolog2) or Suz (suppressor of zeste)12 and  $\beta$ -catenin from extracts of confluent VEC (vascular endothelial cadherin)-null and VEC-positive endothelial cells (ECs). **B**, Quantitative real-time polymerase chain reaction (qRT-PCR) for the TSS of *claudin-5*, *VE-PTP*, and *vWf* performed on endogenous Ezh2-bound chromatin immunoprecipitated from confluent VEC-positive and VEC-null ECs expressing dominant negative form of Tcf4 (TCF4-DN) or GFP (green fluorescent protein; negative control). Inset: WB analysis of TCF4-DN and Ezh2 in extracts from confluent VEC-positive and VEC-null ECs expressing TCF4-DN or control GFP. Vinculin is the loading control. \* $P < 0.05$ ; \*\* $P < 0.01$ ,  $t$  test VEC-null GFP vs VEC-null TCF4-DN. IP indicates immunoprecipitation; and TL, total cell lysate.

and Suz12 (Figure 4A). Surprisingly, we detected a strong Ezh2/ $\beta$ -catenin association in VEC-positive confluent cells that was unlikely to be connected to the analyzed recruitment mechanism (Figure 4A, left). The meaning of this interaction will be further explored in the next section.

$\beta$ -Catenin/FoxO1 association is known to stabilize FoxO1 binding to *claudin-5* promoter. When TCF4-DN (dominant negative form of Tcf4), lacking the  $\beta$ -catenin-interacting region, was overexpressed in VEC-null cells,  $\beta$ -catenin/DNA interaction was abrogated,<sup>5</sup> and Ezh2 binding to *claudin-5*, *VE-PTP*, and *vWf* promoters was strongly weakened (Figure 4B), suggesting a stabilizing role for  $\beta$ -catenin on PcG protein association to target sites.

### VEC Associates With Ezh2 and Sequesters It at the Plasma Membrane

The strong Ezh2/ $\beta$ -catenin association detected in confluent VEC-positive cells (Figure 4A, left) suggested an alternative role for such interaction in this cell type. Indeed, Ezh2 coimmunoprecipitated with endogenous full-length VEC (Figure 5A, left), whereas no interaction was detected between Ezh2 and N-cadherin (Figure 5A, right). Ezh2-VEC interaction was confirmed in vivo in adult mice-derived whole lung extracts (Figure 5B). Biotinylation of cell surface proteins further proved that Ezh2 associates with VEC exposed on the cell membrane (Figure 5C). Moreover, junctional staining of Ezh2 was detected in confluent VEC-positive but not in VEC-null ECs (Figure 5D, arrow). Taken together these data

demonstrate that the observed VEC-Ezh2 interaction sequesters the polycomb protein at the cell surface.

To define whether Ezh2 interacts directly with VEC cytoplasmic tail and which Ezh2 domain is involved in such interaction, we designed a peptide array displaying 20-mers covering the entire amino acid sequence of mouse Ezh2 (746 amino acids). Each peptide spotted on the membrane overlapped the next one by 19 amino acids, resulting in a change of only a single amino acid per peptide and providing a high resolution in determining the interaction sites. Such peptide array was probed with glutathione *S*-transferase (GST)-tagged VEC cytoplasmic tail<sup>26</sup> and free GST as control for nonspecific interactions (Online Figure IXA and IXB). Peptides corresponding to the spots displaying high signal in VEC cytoplasmic tail-probed array and no or low signal in GST-probed control (Online Figure IXB, red dots) were synthesized as biotinylated and used in streptavidin pull-down experiments to confirm protein interactions (Figure 6A). Peptides M6 and M10 corresponding to amino acids 450 to 469 and 454 to 473, respectively, were identified as the sites of Ezh2/VEC direct interaction (Figure 6A and 6B).

We then investigated the role of VEC cytoplasmic partner  $\beta$ -catenin in such interaction. Ezh2/VEC association was reduced in a  $\beta$ -catenin-null EC line ( $\beta$ -catenin knockout) compared with its wild-type counterpart ( $\beta$ -catenin wild type; Figure 6C and 6D). When VEC-null cells were reconstituted with a truncated mutant of VEC lacking the  $\beta$ -catenin-binding domain ( $\Delta\beta$ cat),<sup>5</sup> thus unable to sequester  $\beta$ -catenin at the membrane, VEC displayed a marked reduction of Ezh2

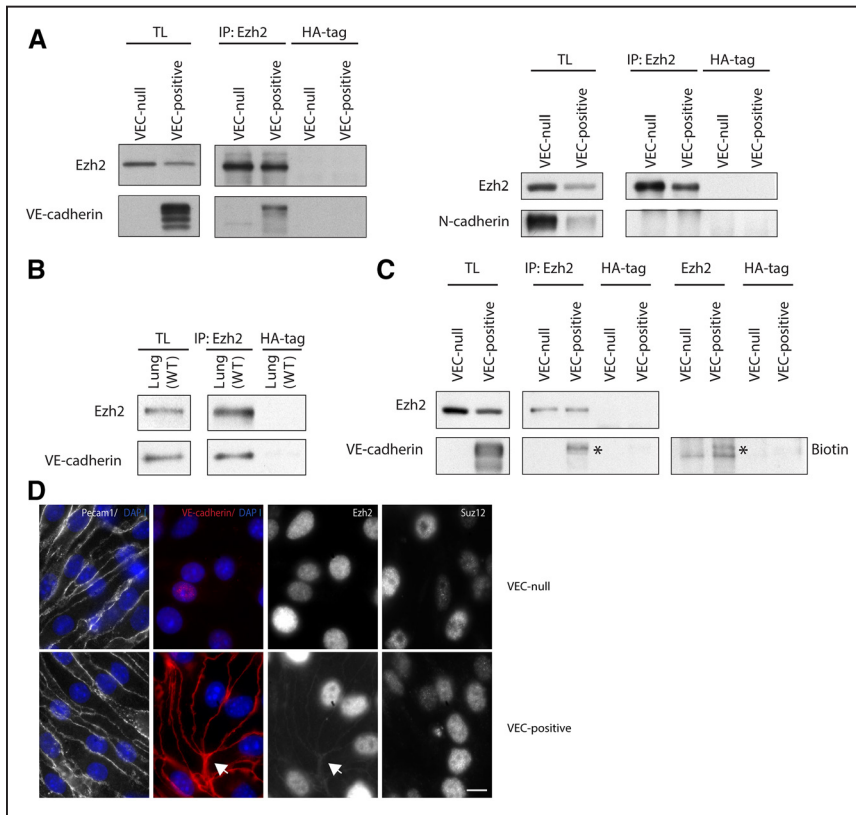


**Figure 5. VEC (vascular endothelial cadherin) sequesters Ezh2 (enhancer of zeste homolog 2) at the plasma membrane.** **A**, Coimmunoprecipitation and WB of endogenous Ezh2 and VEC or N-cadherin from extracts of confluent VEC-null and VEC-positive endothelial cells (ECs). **B**, Coimmunoprecipitation and Western blot (WB) of endogenous Ezh2 and VEC from wild-type (WT) murine whole lung extracts. **C**, Coimmunoprecipitation and WB of endogenous Ezh2 and VEC from extracts of confluent VEC-null and VEC-positive ECs after biotinylation of cell surface proteins. Asterisk highlights Ezh2-associated total and surface VEC bands. **D**, Immunofluorescence analysis of Ezh2 junctional localization (arrow) in confluent VEC-null and VEC-positive ECs. Junctional Suz (suppressor of zeste)12 was not detected. Platelet/endothelial cell adhesion molecule-1 (Pecam1) and VEC were used as junctional markers. Scale bar: 10  $\mu$ m. IP indicates immunoprecipitation; and TL, total cell lysate.

binding (Figure 6G and 6H). These results strongly suggested that  $\beta$ -catenin association to VEC cytoplasmic tail is required for optimal Ezh2 junctional recruitment. Ezh2 peptide array was probed with GST-tagged  $\beta$ -catenin (Online Figure IXC). Biotinylated peptide pull-down with peptides corresponding to the spots displaying high signal in  $\beta$ -catenin-probed array and no or low signal in GST-probed control (Online Figure IXC, red dots) confirmed Ezh2 interaction with  $\beta$ -catenin at amino acids 522 to 541 and 585 to 604, corresponding to peptides O4 and P30 (Figure 6E and 6F).

Ezh2 also associated with another constituent of VEC cytoplasmic junctional complex, p120-catenin (Online Figure X). VEC-null cells reconstituted with a mutant version of VEC lacking the juxtamembrane p120-catenin binding region showed a marked reduction of VEC/Ezh2 interaction (Figure 6G and 6H), suggesting a role for p120-catenin in such association. Ezh2 peptide array was probed with GST-tagged p120-catenin, and the identified putative interacting peptides (Online Figure IXD, red dots) were selected for validation by biotinylated peptide pull-down (Figure 6I). Amino acids 652 to 671, corresponding to peptide R23, were identified as Ezh2 interaction site with p120-catenin (Figure 6I and 6J).

Overall, these data prove that Ezh2 interacts with VEC junctional complex at multiple sites. Whether the identified interactions correspond to different junctional pools of Ezh2 or a single complex is formed is a matter of future investigation.

### Inhibition of Ezh2/VEC Interaction Downregulates Claudin-5, VE-PTP, and vWf Expression

To understand whether Ezh2 sequestration at AJs impacts the expression of *claudin-5*, *VE-PTP*, and *vWf*, we aimed at inhibiting Ezh2/VEC and Ezh2/ $\beta$ -catenin interactions. Selected Ezh2

peptides M6-M10 (VEC-binding sites) and O4-P30 ( $\beta$ -catenin-binding sites) were synthesized in tandem with transactivator of transcription (TAT) of human immunodeficiency virus, to allow peptide entry into the cell. Such TAT-conjugated peptides are expected to bind VEC or  $\beta$ -catenin engaging the domains needed for Ezh2 interaction, thus acting in a dominant negative fashion to inhibit Ezh2 junctional recruitment. VEC-positive cells were treated from subconfluent state throughout the period of time needed to establish AJs to saturate Ezh2-binding sites before the polycomb protein could localize at cell-cell contacts. Treatment with peptides TAT-P30 and TAT-M10 reduced VEC/Ezh2 association by 28% and 45.3%, respectively (Figure 7A). This caused an increase in Ezh2 recruitment to the TSS of *claudin-5*, *VE-PTP*, and *vWf* (Figure 7B), which, in the case of TAT-M10 treatment, corresponded to a significant repression of gene expression in comparison to treatment with a nonbinding TAT-control peptide (Figure 7C). The lack of gene downregulation after TAT-P30 treatment might be because of interference of this peptide with the correct assembly of the FoxO1/ $\beta$ -catenin/PRC2 complex at gene promoters.

### Polycomb Activity Correlates With Claudin-5, VE-PTP, and vWf Repression In Vivo

To verify whether the inhibition of PRC2 activity could enhance the expression of the identified endothelial genes in vivo, we analyzed the effect of Ezh2/Ezh1 inhibition in mouse pups by pharmacological treatment with UNC1999. As reported in Figure 8A, drug administration increased *VE-PTP* and *vWf* expression in lung ECs, but was unable to increase *claudin-5* expression over physiological levels.

EZH2 overexpression is frequent in tumor cells and in vessels of human epithelial ovarian cancers and is associated

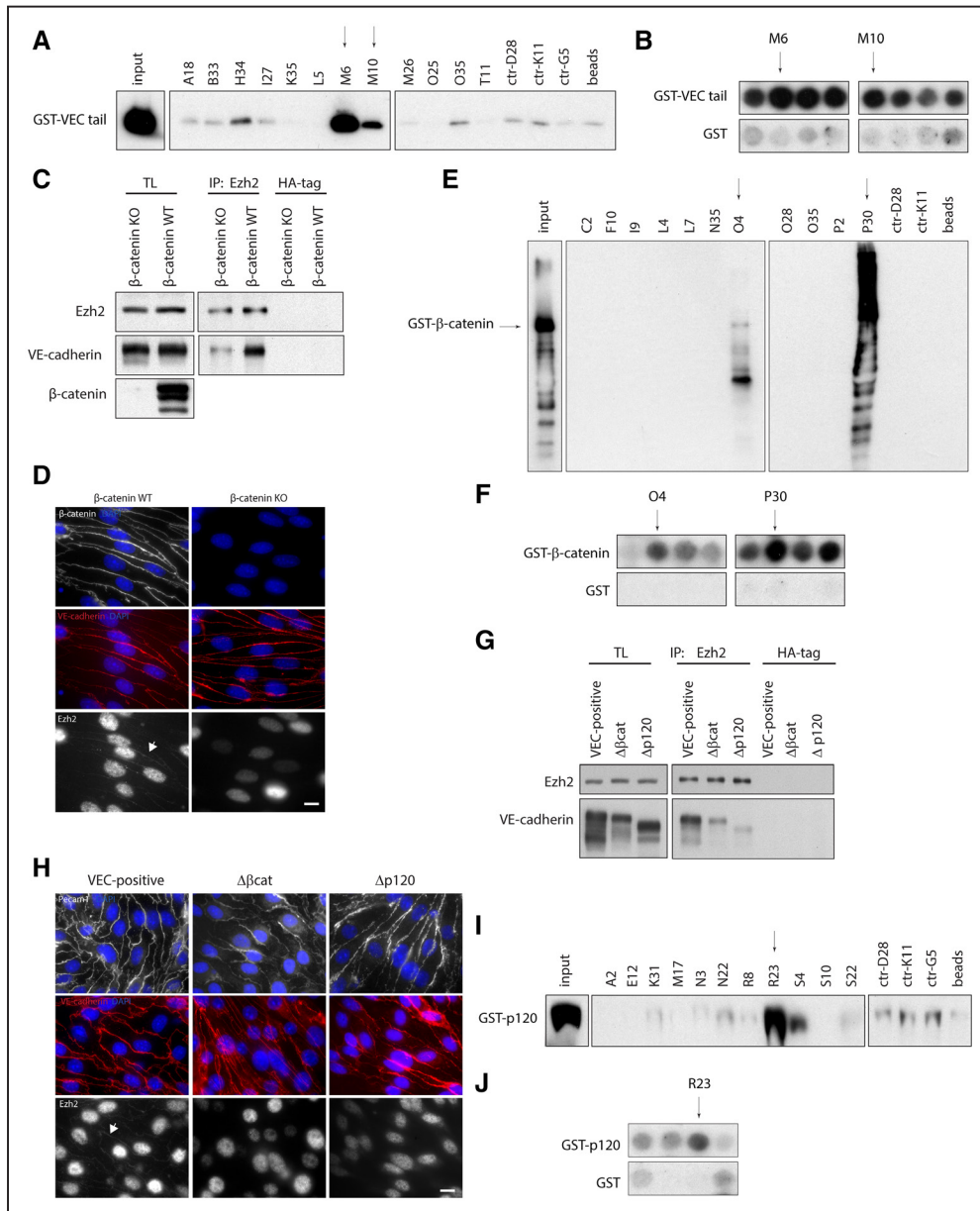


**Figure 6. Analysis of Ezh2 (enhancer of zeste homolog 2) interaction with VEC (vascular endothelial cadherin) junctional complex.** **A**, Streptavidin pull-down of selected biotinylated Ezh2 peptides and GST-tagged VEC cytoplasmic tail. GST-VEC cytoplasmic tail (400 ng) was loaded as input. Peptides displaying no interaction in peptide array were used as controls. Arrows indicate peptides showing positive signal. **B**, Regions of peptide array in the Online Figure IXA and IXB corresponding to selected peptides in (A). **C**, Coimmunoprecipitation and Western blot (WB) of Ezh2 and VEC from extracts of confluent  $\beta$ -catenin knockout (KO) and  $\beta$ -catenin wild-type (WT) endothelial cells (ECs). **D**, Immunofluorescence analysis of Ezh2 (arrow) and  $\beta$ -catenin junctional localization in confluent  $\beta$ -catenin KO and  $\beta$ -catenin WT ECs. VE-cadherin (red) was used as junctional marker. **E**, Streptavidin pull-down of selected biotinylated Ezh2 peptides and GST-tagged  $\beta$ -catenin. GST- $\beta$ -catenin (400 ng) was loaded as input. Peptides displaying no interaction in peptide array were used as controls. Arrows indicate peptides showing positive signal. **F**, Regions of peptide array in the Online Figure IXA and IXC corresponding to selected peptides in (E). **G**, Coimmunoprecipitation and WB of Ezh2 and VEC from extracts of confluent VEC-positive,  $\Delta\beta$ cat, and  $\Delta p120$  ECs. **H**, Immunofluorescence analysis of Ezh2 junctional localization (arrow) in confluent VEC-positive,  $\Delta\beta$ cat, and  $\Delta p120$  ECs. VEC and platelet/endothelial cell adhesion molecule-1 (Pecam1) were used as junctional markers. **I**, Streptavidin pull-down of selected biotinylated Ezh2 peptides and GST-tagged p120-catenin. GST-p120-catenin (300 ng) was loaded as input. Peptides displaying no interaction in peptide array were used as controls. Arrow indicates peptide showing positive signal. **J**, Regions of peptide array in the Online Figure IXA and IXD corresponding to selected peptides in (I). In (D) and (H), scale bar: 10  $\mu$ m. GST indicates glutathione S-transferase; HA, human influenza hemagglutinin; IP, immunoprecipitation; and TL, total cell lysate.

with poor prognosis.<sup>31</sup> Vessels of human healthy ovarian tissue presented very low EZH2 expression, while VEC, Claudin-5, and PECAM1 were clearly detectable (Figure 8B, upper). In contrast, in tumor vasculature, high nuclear EZH2 staining paralleled a significant reduction in VEC and Claudin-5,

whereas PECAM1 expression was unaltered (Figure 8B, lower, and 8C). EC-associated vWf staining was highly variable in both healthy ovarian tissue and tumor samples, preventing a quantitative evaluation of its expression. VE-PTP staining quantification also presented problems of antibody specificity.

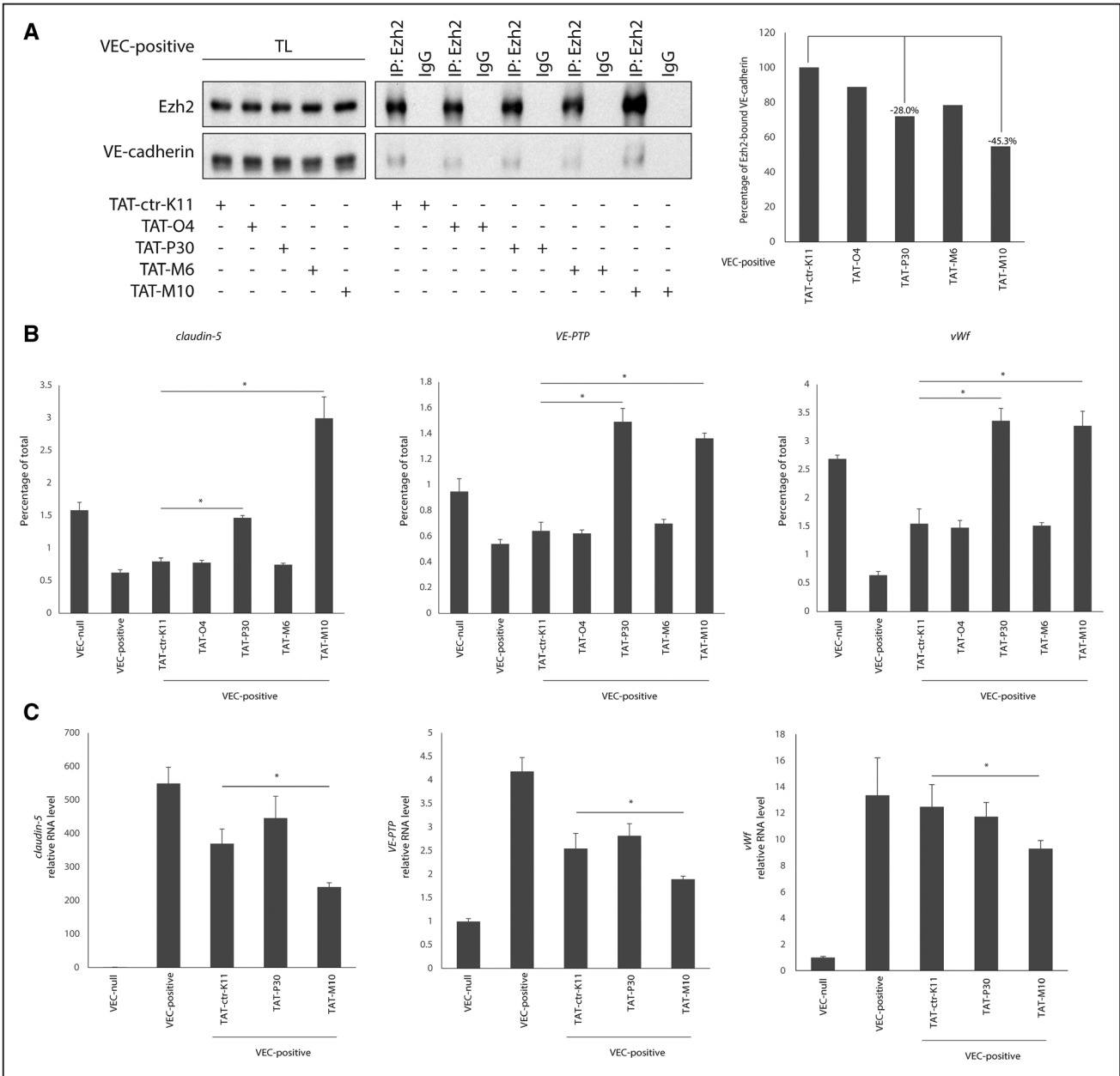


**Figure 7. Inhibition of Ezh2 (enhancer of zeste homolog 2)/VEC (vascular endothelial cadherin) interaction causes *claudin-5*, vascular endothelial-protein tyrosine phosphatase (VE-PTP), and von Willebrand factor (*vWf*) downregulation. A**, Coimmunoprecipitation and Western blot (WB) of endogenous Ezh2 and VEC from extracts of VEC-positive endothelial cells (ECs) treated with VEC-binding transactivator of transcription (TAT)-M6 and TAT-M10 peptides,  $\beta$ -catenin-binding TAT-O4 and TAT-P30 peptides or nonbinding TAT-ctr-K11 peptide as control (left). Quantification of coprecipitated VEC protein normalized on precipitated Ezh2 level (right). **B**, Quantitative real-time polymerase chain reaction (qRT-PCR) for the transcription start site (TSS) of *claudin-5*, *VE-PTP*, and *vWf* performed on endogenous Ezh2-bound chromatin immunoprecipitated from VEC-positive ECs treated with VEC-binding TAT-M6 and TAT-M10 peptides,  $\beta$ -catenin-binding TAT-O4 and TAT-P30 peptides or nonbinding TAT-ctr-K11 peptide as control. Levels of DNA are normalized to input; columns are means $\pm$ SD of triplicates from a representative experiment. \* $P$ <0.01,  $t$  test TAT-ctr-K11 vs TAT-P30 or TAT-M10 treatment. **C**, qRT-PCR analysis of *claudin-5*, *VE-PTP*, and *vWf* expression in VEC-positive ECs treated with VEC-binding TAT-M10 peptide,  $\beta$ -catenin-binding TAT-P30 peptide or nonbinding TAT-ctr-K11 peptide as control. Levels of mRNA are normalized to GAPDH; columns are means $\pm$ SEM of triplicates from a representative experiment. \* $P$ <0.01,  $t$  test TAT-ctr-K11 vs. TAT-M10 treatment. IP indicates immunoprecipitation; and TL, total cell lysate.

Nonetheless, a reduction of VE-PTP signal could be appreciated in tumor vessels (Online Figure XI).

### Discussion

In this study, we describe a novel mechanism through which VEC expression and clustering upregulate endothelial-specific

genes and contribute to endothelial differentiation and stability. We found that VEC engagement at cell-cell contacts acts by inhibiting PcG protein-mediated epigenetic modifications of EC chromatin. PcG proteins have been implicated in several developmental processes,<sup>7,8</sup> and Ezh2 activity was claimed to be involved in the regulation of genes important in tumor

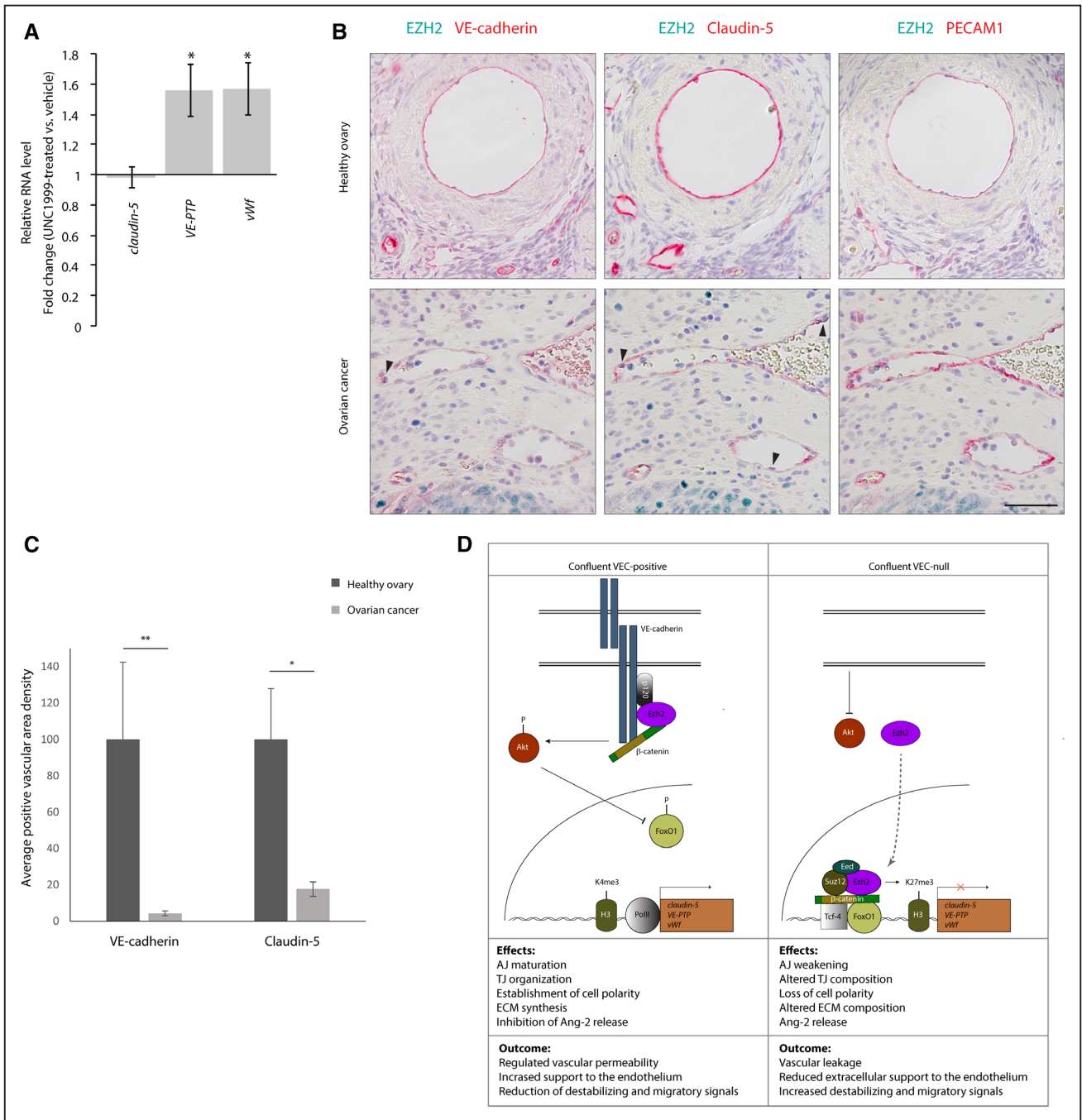


**Figure 8. Ezh2 (enhancer of zeste homolog 2) activity correlates with *claudin-5*, vascular endothelial-protein tyrosine phosphatase (*VE-PTP*), and von Willebrand factor (*vWf*) repression in vivo.** **A**, Quantitative real-time polymerase chain reaction (qRT-PCR) analysis of *claudin-5*, *VE-PTP*, and *vWf* expression in lungs of vehicle- or UNC1999-treated pups (P6). Data are represented as fold change of UNC1999 treated vs vehicle and are means±SD from at least 4 mice per group. Gene expression was normalized to *VEC* (vascular endothelial cadherin) expression. **B**, Immunohistochemistry (IHC) staining of VEC, Claudin-5, platelet/endothelial cell adhesion molecule-1 (PECAM1; red) and EZH2 (green) expression in serial sections of human healthy ovary (**upper**) or serous surface papillary ovarian carcinoma (**lower**). Black arrowheads point to tumor vessel endothelial cells (ECs) expressing high levels of EZH2. Scale bar: 50 μm. **C**, Quantification of IHC stainings in (**B**). For VEC and claudin-5, areas of specific signal, divided by the total measured area, were normalized to the corresponding values of PECAM1 staining. Columns are means±SEM (n=3 healthy ovaries; 4 ovarian carcinomas; at least 3 fields per sample). **D**, Suggested model for the regulation of *claudin-5*, *VE-PTP*, and *vWf* genes. Clustered VEC recruits β-catenin and activates Akt leading to FoxO1 (Forkhead box protein O1) phosphorylation and inhibition.<sup>5</sup> Furthermore, Ezh2 is sequestered at the cell membrane by association with VEC cytoplasmic tail (**left**). These mechanisms allow gene activation by impeding the recruitment of PcG (polycomb group) proteins to gene promoters. Claudin-5 expression allows the correct organization of tight junctions (TJs) and regulation of vessel permeability.<sup>5,27</sup> VE-PTP regulates adherens junction (AJ) maturation<sup>28</sup> and VEGFR2 (vascular endothelial growth factor receptor-2) activity,<sup>13,29</sup> whereas vWf contributes to extracellular matrix (ECM) formation and inhibits Ang (angiopoietin)-2 release.<sup>14,30</sup> These effects are likely to contribute to vessel stabilization and prevent vascular leakage. In (**A**) and (**C**), \*P<0.05; \*\*P<0.01, t test.

Downloaded from <http://circres.ahajournals.org/> by guest on January 23, 2018

angiogenesis and Kaposi Sarcoma.<sup>31</sup> Furthermore, Ezh2 was reported to play a role in maintaining vascular integrity during embryonic development.<sup>32</sup>

However, these studies mainly focused on the effects of Ezh2 inhibition without investigating in detail the mechanisms of polycomb regulation in ECs. We observed that VEC expression and clustering were able to trigger a gene expression program contributing to endothelial differentiation. Some of these endothelial genes seemed to be regulated by polycomb activity, thus pointing to a possible central role of VEC/polycomb crosstalk in orchestrating endothelial specification.

Within the set of genes upregulated by VEC, we selected endothelial-specific *claudin-5*, *VE-PTP*, and *vWf*. Claudin-5 is a major component of endothelial TJs and determines size and charge selectivity of endothelial paracellular permeability.<sup>4,5,27,33</sup>

VE-PTP exerts different context-specific activities including associating with VEC and reducing its tyrosine phosphorylation.<sup>34</sup> Absence of VE-PTP impairs AJ maturation, inducing vessel destabilization and increased permeability.<sup>28,35</sup> VE-PTP associates with Tie-2 receptor modulating Ang (angiopoietin) signaling<sup>36</sup> and interacts with VEGFR2 (vascular endothelial growth factor receptor-2) limiting its signaling activity.<sup>13,29</sup>

vWf is a crucial component of EC extracellular matrix that provides mechanical support to the EC monolayer<sup>30</sup> and limits the release of vessel-destabilizing Ang-2 from endothelial Weibel–Palade bodies.<sup>14</sup> Consistent with our data, a larger pool of vWf is present in confluent ECs compared with subconfluent condition.<sup>37</sup>

Although our analysis was mainly focused on these 3 genes, other genes regulated by VEC are involved in inhibition of cell proliferation, decrease of sprouting angiogenesis, promotion of cell adhesion, and production of extracellular matrix, suggesting a broader role of VEC expression and clustering in inducing vessel stabilization.

We previously found<sup>5</sup> that VEC expression derepresses the endothelial-specific gene *claudin-5* by restraining the activity of FoxO1 and  $\beta$ -catenin.<sup>33</sup> Here, we show that nuclear FoxO1 and  $\beta$ -catenin increase polycomb targeting to the promoter regions of a set of endothelial genes. We observed that induction of *claudin-5*,<sup>5</sup> *VE-PTP*, and *vWf* relies on VEC capacity to activate the PI3K/AKT pathway, leading to FoxO1 inactivation,<sup>4</sup> and to sequester  $\beta$ -catenin at the cell membrane. The absence of VEC clustering prevented the expression of this set of genes. The work presented here confirms and extends what previously observed for *claudin-5*<sup>5</sup> and further underlines the role of FoxO1 as a key transcription factor in endothelial differentiation and homeostasis.<sup>38</sup> This is in agreement with a recent report highlighting a key role of Akt1 activation and FoxO inhibition in stabilizing the endothelial barrier and preventing vascular leakage.<sup>39</sup>

Little is known about the molecular mechanisms of FoxO1-mediated gene repression. We found that FoxO1 physically associates with PcG proteins and, through still unknown mechanisms, contributes to their association to a selected set of endothelial gene promoters inducing chromatin conformational changes and gene inhibition.  $\beta$ -Catenin takes part in such multiprotein complex and stabilizes PcG protein binding

to DNA, as TCF4-DN-mediated abrogation of  $\beta$ -catenin/DNA binding destabilizes Ezh2/promoter interaction.

PcG proteins have been previously reported to have atypical extranuclear localizations.<sup>40,41</sup> We show here that VEC also reduces polycomb nuclear activity by sequestering Ezh2 at the plasma membrane in a  $\beta$ -catenin-dependent and p120-catenin-dependent manner. Ezh2 interaction with VEC was confirmed in vivo in mouse lung extracts in the absence of any crosslinking reaction, whereas no association was detected between Ezh2 and the other major classical endothelial cadherin, N-cadherin, likely as a result of the reduced binding of this adhesion molecule to p120-catenin.<sup>42</sup> Recently, EZH2 has been shown to interact with  $\beta$ -catenin in liver cancer stem cells<sup>43</sup> through its N-terminal domain (amino acids 1–334). This was defined by domain mapping assays using EZH2 truncation mutants. Our analysis identified the Ezh2 sites of direct interaction with  $\beta$ -catenin in the domain comprised between amino acids 522 and 604. Deletion of domain 1 to 334 might alter the protein structural integrity, affecting EZH2/ $\beta$ -catenin interaction at downstream residues.

Ezh2/VEC association was shown to play a functional role in regulating gene expression. Inhibition of such interaction, and likely the consequent release of Ezh2 protein in the cytoplasm, increased its recruitment to *claudin-5*, *VE-PTP*, and *vWf* gene promoters causing their downregulation. The strong increase of Ezh2 recruitment at gene promoters, however, did not parallel a similarly strong repression of gene expression.

This was likely because of reduced FoxO1 and  $\beta$ -catenin nuclear abundance in the confluent VEC-positive condition, impeding the correct assembly of the nuclear repressive complex.

Thus, we propose that an event happening at cell–cell contacts, that is, VEC clustering, triggers and orchestrates a network of pathways and epigenetic events, regulating several aspects of endothelial homeostasis and vascular stability (Figure 8D).

Pharmacological inhibition of Ezh2/Ezh1 led to the upregulation of *VE-PTP* and *vWf* in mouse pups, confirming that these genes are dependent on polycomb activity in vivo. *Claudin-5* was not significantly upregulated by such treatment, likely because its expression is unable to increase over a physiological threshold. Additional studies are needed for understanding the kinetics of expression of this gene in the presence or absence of polycombs in different vascular regions.

Deregulated angiogenesis is a characteristic of several human pathologies and is a hallmark of cancer. Tumor vessels present altered endothelial cell–cell junctions, are hyperpermeable, have low pericyte coverage, and altered basement membrane composition and stiffness. Tumor vessel stabilization by increased VEC has been shown to reduce tumor metastasis.<sup>44,45</sup> Ezh2 expression is increased in tumor-associated ECs, and this has been linked to increased vascular density and reduced vessel maturation.<sup>31</sup> Our results show that reduced VEC and increased EZH2 nuclear staining in human ovarian carcinoma vessels parallel the downregulation of *Claudin-5* and *VE-PTP*, suggesting a possible alteration of the identified signaling mechanism.

In conclusion, this work introduces a novel role for VEC in the regulation of polycomb activity and, consequently, EC

differentiation and vascular maturation. The available genetic and pharmacological approaches to inhibit polycomb function will be instrumental to identify the role of this mechanism in different pathological conditions of the vascular system and to investigate new therapeutic opportunities to induce vessel normalization in cancer.<sup>4</sup>

### Acknowledgments

We thank Luca Ferrarini for help in bioinformatic analysis, Djamil A. Damry for scientific input, and Emanuele Martini and Dario Parazzoli for imaging analysis. The anti-vascular endothelial-protein tyrosine phosphatase (VE-PTP; hPTPb1-8) antibody and FKHR-TM (Forkhead transcription factor triple mutant) adenovirus were kind gifts of Dietmar Vestweber and Christopher Daly, respectively.

### Sources of Funding

This work was supported by the Francis Crick Institute which receives its core funding from Cancer Research UK (FC001057), the UK Medical Research Council (FC001057), and the Wellcome Trust (FC001057); by Associazione Italiana per la Ricerca sul Cancro (AIRC; investigator grant [IG] 16683), AIRC IG2016 18683 and Special Program Molecular Clinical Oncology 5x1000 to AGIMM (AIRC Gruppo Italiano Malattie Mieloproliferative; 10005); by the European Research Council (project EC-ERC-VEPC contract 742922); by ITN (initial training networks) BtRAIN grant 675619; by CARIPLO Foundation (2008.2463) and TELETHON (GGP14149). Research was also supported by the grants R01CA218600, R01GM122749, and R01HD088626 (to J. Jin) from the US National Institutes of Health. Sequencing was performed by the SNP&SEQ Technology platform in Uppsala. The facility is part of the National Genomics Infrastructure (NGI) Sweden and Science for Life Laboratory. The SNP&SEQ Platform is also supported by the Swedish Research Council and the Knut and Alice Wallenberg Foundation. E. Dejana is supported by the Swedish Science Council and the Knut and Alice Wallenberg Foundation.

### Disclosures

None.

### References

- Carmeliet P, Jain RK. Principles and mechanisms of vessel normalization for cancer and other angiogenic diseases. *Nat Rev Drug Discov*. 2011;10:417–427. doi: 10.1038/nrd3455.
- Baluk P, Morikawa S, Haskell A, Mancuso M, McDonald DM. Abnormalities of basement membrane on blood vessels and endothelial sprouts in tumors. *Am J Pathol*. 2003;163:1801–1815. doi: 10.1016/S0002-9440(10)63540-7.
- Giannotta M, Trani M, Dejana E. VE-cadherin and endothelial adherens junctions: active guardians of vascular integrity. *Dev Cell*. 2013;26:441–454. doi: 10.1016/j.devcel.2013.08.020.
- Dejana E, Giampietro C. Vascular endothelial-cadherin and vascular stability. *Curr Opin Hematol*. 2012;19:218–223. doi: 10.1097/MOH.0b013e3283523e1c.
- Taddei A, Giampietro C, Conti A, Orsenigo F, Breviaro F, Pirazzoli V, Potente M, Daly C, Dimmeler S, Dejana E. Endothelial adherens junctions control tight junctions by VE-cadherin-mediated upregulation of claudin-5. *Nat Cell Biol*. 2008;10:923–934. doi: 10.1038/ncb1752.
- Simon JA, Kingston RE. Mechanisms of polycomb gene silencing: knowns and unknowns. *Nat Rev Mol Cell Biol*. 2009;10:697–708. doi: 10.1038/nrm2763.
- Conway E, Healy E, Bracken AP. PRC2 mediated H3K27 methylations in cellular identity and cancer. *Curr Opin Cell Biol*. 2015;37:42–48. doi: 10.1016/j.ccb.2015.10.003.
- Pasini D, Bracken AP, Jensen MR, Lazzarini Denchi E, Helin K. Suz12 is essential for mouse development and for EZH2 histone methyltransferase activity. *EMBO J*. 2004;23:4061–4071. doi: 10.1038/sj.emboj.7600402.
- Morey L, Helin K. Polycomb group protein-mediated repression of transcription. *Trends Biochem Sci*. 2010;35:323–332. doi: 10.1016/j.tibs.2010.02.009.
- Simon JA, Kingston RE. Occupying chromatin: polycomb mechanisms for getting to genomic targets, stopping transcriptional traffic, and staying put. *Mol Cell*. 2013;49:808–824. doi: 10.1016/j.molcel.2013.02.013.
- Schuettengruber B, Cavalli G. Recruitment of polycomb group complexes and their role in the dynamic regulation of cell fate choice. *Development*. 2009;136:3531–3542. doi: 10.1242/dev.033902.
- Daneman R, Zhou L, Agalliu D, Cahoy JD, Kaushal A, Barres BA. The mouse blood-brain barrier transcriptome: a new resource for understanding the development and function of brain endothelial cells. *PLoS One*. 2010;5:e13741. doi: 10.1371/journal.pone.0013741.
- Küppers V, Vockel M, Nottebaum AF, Vestweber D. Phosphatases and kinases as regulators of the endothelial barrier function. *Cell Tissue Res*. 2014;355:577–586. doi: 10.1007/s00441-014-1812-1.
- Starke RD, Ferraro F, Paschalaki KE, Dryden NH, McKinnon TA, Sutton RE, Payne EM, Haskard DO, Hughes AD, Cutler DF, Laffan MA, Randi AM. Endothelial von Willebrand factor regulates angiogenesis. *Blood*. 2011;117:1071–1080. doi: 10.1182/blood-2010-01-264507.
- Lampugnani MG, Zanetti A, Breviaro F, Balconi G, Orsenigo F, Corada M, Spagnuolo R, Betson M, Braga V, Dejana E. VE-cadherin regulates endothelial actin activating Rac and increasing membrane association of Tiam. *Mol Biol Cell*. 2002;13:1175–1189. doi: 10.1091/mbc.01-07-0368.
- Coma S, Allard-Ratick M, Akino T, van Meeteren LA, Mammoto A, Klagsbrun M. GATA2 and Lmo2 control angiogenesis and lymphangiogenesis via direct transcriptional regulation of neuropilin-2. *Angiogenesis*. 2013;16:939–952. doi: 10.1007/s10456-013-9370-9.
- Dalmaso AP, Goldish D, Benson BA, Tsai AK, Wasilik KR, Vercellotti GM. Interleukin-4 induces up-regulation of endothelial cell claudin-5 through activation of FoxO1: role in protection from complement-mediated injury. *J Biol Chem*. 2014;289:838–847. doi: 10.1074/jbc.M113.455766.
- Dejana E, Taddei A, Randi AM. Foxs and Ets in the transcriptional regulation of endothelial cell differentiation and angiogenesis. *Biochim Biophys Acta*. 2007;1775:298–312. doi: 10.1016/j.bbcan.2007.05.003.
- Fontijn RD, Volger OL, Fledderus JO, Reijerkerk A, de Vries HE, Horrevoets AJ. SOX-18 controls endothelial-specific claudin-5 gene expression and barrier function. *Am J Physiol Heart Circ Physiol*. 2008;294:H891–H900. doi: 10.1152/ajpheart.01248.2007.
- Kofler NM, Shawber CJ, Kangsamaksin T, Reed HO, Galatioto J, Kitajewski J. Notch signaling in developmental and tumor angiogenesis. *Genes Cancer*. 2011;2:1106–1116. doi: 10.1177/1947601911423030.
- Huang TH, Chu TY. Repression of miR-126 and upregulation of adreno-medullin in the stromal endothelium by cancer-stromal cross talks confers angiogenesis of cervical cancer. *Oncogene*. 2014;33:3636–3647. doi: 10.1038/onc.2013.335.
- Nourshargh S, Krombach F, Dejana E. The role of JAM-A and PECAM-1 in modulating leukocyte infiltration in inflamed and ischemic tissues. *J Leukoc Biol*. 2006;80:714–718. doi: 10.1189/jlb.1105645.
- Huang da W, Sherman BT, Lempicki RA. Systematic and integrative analysis of large gene lists using DAVID bioinformatics resources. *Nat Protoc*. 2009;4:44–57. doi: 10.1038/nprot.2008.211.
- Daly C, Wong V, Burova E, Wei Y, Zabski S, Griffiths J, Lai KM, Lin HC, Ioffe E, Yancopoulos GD, Rudge JS. Angiopoietin-1 modulates endothelial cell function and gene expression via the transcription factor FKHR (FOXO1). *Genes Dev*. 2004;18:1060–1071. doi: 10.1101/gad.1189704.
- Leeb M, Pasini D, Novatchkova M, Jaritz M, Helin K, Wutz A. Polycomb complexes act redundantly to repress genomic repeats and genes. *Genes Dev*. 2010;24:265–276. doi: 10.1101/gad.544410.
- Giampietro C, Disanza A, Bravi L, Barrios-Rodiles M, Corada M, Frittoli E, Savorani C, Lampugnani MG, Boggetti B, Niessen C, Wrana JL, Scita G, Dejana E. The actin-binding protein EPS8 binds VE-cadherin and modulates YAP localization and signaling. *J Cell Biol*. 2015;211:1177–1192. doi: 10.1083/jcb.201501089.
- Nitta T, Hata M, Gotoh S, Seo Y, Sasaki H, Hashimoto N, Furuse M, Tsukita S. Size-selective loosening of the blood-brain barrier in claudin-5-deficient mice. *J Cell Biol*. 2003;161:653–660. doi: 10.1083/jcb.200302070.
- Carra S, Foglia E, Cermenati S, Bresciani E, Giampietro C, Lora Lamia C, Dejana E, Beltrame M, Cotelli F. Ve-ptp modulates vascular integrity by promoting adherens junction maturation. *PLoS One*. 2012;7:e51245. doi: 10.1371/journal.pone.0051245.
- Hayashi M, Majumdar A, Li X, et al. VE-PTP regulates VEGFR2 activity in stalk cells to establish endothelial cell polarity and lumen formation. *Nat Commun*. 2013;4:1672. doi: 10.1038/ncomms2683.
- Ruggeri ZM. The role of von Willebrand factor in thrombus formation. *Thromb Res*. 2007;120(suppl 1):S5–S9. doi: 10.1016/j.thromres.2007.03.011.

31. Lu C, Han HD, Mangala LS, et al. Regulation of tumor angiogenesis by EZH2. *Cancer Cell*. 2010;18:185–197. doi: 10.1016/j.ccr.2010.06.016.
32. Delgado-Olguín P, Dang LT, He D, Thomas S, Chi L, Sukonnik T, Khyzha N, Dobenecker MW, Fish JE, Bruneau BG. Ezh2-mediated repression of a transcriptional pathway upstream of Mmp9 maintains integrity of the developing vasculature. *Development*. 2014;141:4610–4617. doi: 10.1242/dev.112607.
33. Beard RS Jr, Haines RJ, Wu KY, Reynolds JJ, Davis SM, Elliott JE, Malinin NL, Chatterjee V, Cha BJ, Wu MH, Yuan SY. Non-muscle Mlck is required for  $\beta$ -catenin- and FoxO1-dependent downregulation of Cldn5 in IL-1 $\beta$ -mediated barrier dysfunction in brain endothelial cells. *J Cell Sci*. 2014;127:1840–1853. doi: 10.1242/jcs.144550.
34. Nawroth R, Poell G, Ranft A, Kloep S, Samulowitz U, Fachinger G, Golding M, Shima DT, Deutsch U, Vestweber D. VE-PTP and VE-cadherin ectodomains interact to facilitate regulation of phosphorylation and cell contacts. *EMBO J*. 2002;21:4885–4895.
35. Nottebaum AF, Cagna G, Winderlich M, Gamp AC, Linnepe R, Polaschegg C, Filippova K, Lyck R, Engelhardt B, Kamenyeva O, Bixel MG, Butz S, Vestweber D. VE-PTP maintains the endothelial barrier via plakoglobin and becomes dissociated from VE-cadherin by leukocytes and by VEGF. *J Exp Med*. 2008;205:2929–2945. doi: 10.1084/jem.20080406.
36. Saharinen P, Eklund L, Miettinen J, Wirkkala R, Anisimov A, Winderlich M, Nottebaum A, Vestweber D, Deutsch U, Koh GY, Olsen BR, Alitalo K. Angiopoietins assemble distinct Tie2 signalling complexes in endothelial cell-cell and cell-matrix contacts. *Nat Cell Biol*. 2008;10:527–537. doi: 10.1038/ncb1715.
37. Howell GJ, Herbert SP, Smith JM, Mittar S, Ewan LC, Mohammed M, Hunter AR, Simpson N, Turner AJ, Zachary I, Walker JH, Ponnambalam S. Endothelial cell confluence regulates Weibel-Palade body formation. *Mol Membr Biol*. 2004;21:413–421. doi: 10.1080/09687860400011571.
38. Wilhelm K, Happel K, Eelen G, et al. FOXO1 couples metabolic activity and growth state in the vascular endothelium. *Nature*. 2016;529:216–220. doi: 10.1038/nature16498.
39. Gao F, Artham S, Sabbineni H, Al-Azayzih A, Peng XD, Hay N, Adams RH, Byzova TV, Somanath PR. Akt1 promotes stimuli-induced endothelial-barrier protection through FoxO-mediated tight-junction protein turnover. *Cell Mol Life Sci*. 2016;73:3917–3933. doi: 10.1007/s00018-016-2232-z.
40. Witte V, Laffert B, Rosorius O, Lischka P, Blume K, Galler G, Stilper A, Willbold D, D'Aloja P, Sixt M, Kolanus J, Ott M, Kolanus W, Schuler G, Baur AS. HIV-1 Nef mimics an integrin receptor signal that recruits the polycomb group protein Eed to the plasma membrane. *Mol Cell*. 2004;13:179–190.
41. Su IH, Dobenecker MW, Dickinson E, Oser M, Basavaraj A, Marqueron R, Viale A, Reinberg D, Wülfing C, Tarakhovskiy A. Polycomb group protein ezh2 controls actin polymerization and cell signaling. *Cell*. 2005;121:425–436. doi: 10.1016/j.cell.2005.02.029.
42. Giampietro C, Taddei A, Corada M, Sarra-Ferraris GM, Alcalay M, Cavallaro U, Orsenigo F, Lampugnani MG, Dejana E. Overlapping and divergent signaling pathways of N-cadherin and VE-cadherin in endothelial cells. *Blood*. 2012;119:2159–2170. doi: 10.1182/blood-2011-09-381012.
43. Zhu P, Wang Y, Huang G, Ye B, Liu B, Wu J, Du Y, He L, Fan Z. Inc- $\beta$ -Catm elicits EZH2-dependent  $\beta$ -catenin stabilization and sustains liver CSC self-renewal. *Nat Struct Mol Biol*. 2016;23:631–639. doi: 10.1038/nsmb.3235.
44. Mazzone M, Dettori D, de Oliveira RL, et al. Heterozygous deficiency of PHD2 restores tumor oxygenation and inhibits metastasis via endothelial normalization. *Cell*. 2009;136:839–851. doi: 10.1016/j.cell.2009.01.020.
45. Zhao Y, Ting KK, Li J, et al. Targeting vascular endothelial-cadherin in tumor-associated blood vessels promotes T-cell-mediated immunotherapy. *Cancer Res*. 2017;77:4434–4447. doi: 10.1158/0008-5472.CAN-16-3129.

# Circulation Research

JOURNAL OF THE AMERICAN HEART ASSOCIATION



## VE-Cadherin–Mediated Epigenetic Regulation of Endothelial Gene Expression

Marco F. Morini, Costanza Giampietro, Monica Corada, Federica Pisati, Elisa Lavarone, Sara I. Cunha, Lei L. Conze, Nicola O'Reilly, Dhira Joshi, Svend Kjaer, Roger George, Emma Nye, Anqi Ma, Jian Jin, Richard Mitter, Michela Lupia, Ugo Cavallaro, Diego Pasini, Dinis P. Calado, Elisabetta Dejana and Andrea Taddei

*Circ Res.* 2018;122:231-245; originally published online December 12, 2017;  
doi: 10.1161/CIRCRESAHA.117.312392

*Circulation Research* is published by the American Heart Association, 7272 Greenville Avenue, Dallas, TX 75231  
Copyright © 2017 American Heart Association, Inc. All rights reserved.  
Print ISSN: 0009-7330. Online ISSN: 1524-4571

The online version of this article, along with updated information and services, is located on the  
World Wide Web at:

<http://circres.ahajournals.org/content/122/2/231>

Free via Open Access

Data Supplement (unedited) at:

<http://circres.ahajournals.org/content/suppl/2017/12/11/CIRCRESAHA.117.312392.DC1>

**Permissions:** Requests for permissions to reproduce figures, tables, or portions of articles originally published in *Circulation Research* can be obtained via RightsLink, a service of the Copyright Clearance Center, not the Editorial Office. Once the online version of the published article for which permission is being requested is located, click Request Permissions in the middle column of the Web page under Services. Further information about this process is available in the [Permissions and Rights Question and Answer](#) document.

**Reprints:** Information about reprints can be found online at:  
<http://www.lww.com/reprints>

**Subscriptions:** Information about subscribing to *Circulation Research* is online at:  
<http://circres.ahajournals.org/subscriptions/>

## SUPPLEMENTAL MATERIAL

### VE-cadherin-mediated Epigenetic Regulation of Endothelial Gene Expression

M. F. Morini, C. Giampietro, M. Corada, F. Pisati, E. Lavarone, S. I. Cunha, L. L. Conze, N. O'Reilly, D. Joshi, S. Kjaer, R. George, E. Nye, A. Ma, J. Jin, R. Mitter, M. Lupia, U. Cavallaro, D. Pasini, D. P. Calado, E. Dejana and A. Taddei

### DETAILED METHODS

#### Data Disclosure

The data that support the findings of this study are available from the corresponding author upon reasonable request.

#### Cell culture

The cell lines used in this study were:

- ECs derived from murine embryonic stem cells with homozygous null mutation of the *VEC* gene (*VEC*-null)<sup>1</sup>. The wild type form of *VEC* was introduced in these cells (*VEC*-positive) using retrovirus-mediated transfer as described in detail by Lampugnani et al.<sup>2</sup>;
- $\Delta\beta$ cat cells, ECs expressing a truncated mutant of *VEC* (lacking residues 703-784 of human *VEC*)<sup>3</sup>, which correspond to the  $\beta$ -catenin-binding region<sup>2</sup>;
- $\Delta p120$  cells, ECs expressing a truncated mutant of *VEC* (lacking residues 621-702 of human *VEC*), which correspond to the p120-catenin-binding region<sup>2</sup>;
- IL2-*VEC* cells, ECs expressing a mutated version of *VEC* made up of the *VEC* cytoplasmic domain (amino acids 621-784) fused to the extracellular and transmembrane domains of IL-2 receptor  $\alpha$ -chain (from Andrew Kowalczyk, Emory University, Atlanta, GA)<sup>4,5</sup>;
- $\beta$ -Catenin WT and  $\beta$ -catenin KO ECs were derived from lungs of adult  $\beta$ -catenin<sup>flox/flox</sup> mice<sup>6</sup>, immortalized as previously described<sup>1,7</sup> and infected with an adenovirus encoding GFP (control) or CRE recombinase to obtain  *$\beta$ -catenin* gene recombination.

For all ECs of murine origin, culture medium was DMEM (GIBCO) with 20% North American (NA) fetal bovine serum (FBS) (HyClone), glutamine (2 mM; Sigma), penicillin/streptomycin (100 units/l; Sigma), sodium pyruvate (1 mM; Sigma), heparin (100  $\mu$ g/ml, from porcine intestinal mucosa; Sigma), and EC growth supplement (ECGS) (5  $\mu$ g/ml, made in our lab from calf brain) (complete culture medium). Starving medium was MCDB 131 (GIBCO) with 1% bovine serum albumin (BSA) (EuroClone), glutamine (2 mM), penicillin/streptomycin (100 units/l) and sodium pyruvate (1mM).

- Human dermal microvascular endothelial cells-1 (HMEC-1) (from STP Cell Services, The Francis Crick Institute, London, UK) were cultured in MCDB 131 (Thermo Fisher) with 10% North American (NA) fetal bovine serum (FBS) (HyClone), glutamine (10 nM; Sigma), penicillin/streptomycin (100 units/l; Sigma), epidermal growth factor (EGF) (30ng/ml; Sigma) and hydrocortisone (1  $\mu$ g/ml; Sigma);

- 293T-Phoenix-Ecotropic packaging cells were provided by IFOM Cell Culture facility and cultured in DMEM medium supplemented with 10 % South American (SA) FBS (Hyclone), glutamine (2 mM) and sodium pyruvate (1 mM);

- Low passage AD-HEK293 cell line (human embryonic kidney, American Type Culture Collection, Manassas, VA), used for adenoviral production, were provided by IFOM Cell Culture facility and grown in DMEM medium supplemented with 10% FBS NA, glutamine (4 mM), penicillin/streptomycin (100 units/l), and sodium pyruvate (1 mM).

All cells were cultured at 37°C in a humidified atmosphere with 5% CO<sub>2</sub>.

#### Lentiviral and adenoviral preparations

$\Delta N$ - $\beta$ catenin construct was obtained from C. Brancolini (University of Udine, Udine, Italy). Lentiviral vectors used to stably express a short hairpin RNA against *Suz12* (sh-*Suz12*), to overexpress *Suz12* and the respective controls were a kind gift of D. Pasini (IEO, Milan, Italy). Packaging plasmids were kindly donated by L. Naldini (HSR-TIGET, San Raffaele Telethon Institute for Gene Therapy, Milan, Italy).

Lentiviral vectors were produced as described by Dull et al.<sup>8</sup>. Briefly, on day 1, 293T-Phoenix-Ecotropic packaging cells were transfected with the viral genome using calcium phosphate and incubated overnight with the transfection mix. On day 2 the medium containing the transfection mix was removed and 293T-Phoenix-Ecotropic cells were grown in as little medium as possible to concentrate the virus. On day 3 the medium containing the virus was removed, passed through a 0.45 µm diameter filter, supplemented with Polybrene (8 µg/ml, from IFOM Cell Culture facility) and placed on cells to be infected. The same procedure was repeated on day 4. Sh-Suz12- and sh-Empty-infected cells were selected with hygromycin 300 µg/ml. Cells were kept under selection until control non-infected cells died. Suz12-overexpressing cells and their Empty control were selected with Puromycin 3 µg/ml. Cells were kept under selection until control non-infected cells died. The FKHR-TM adenovirus has been previously described<sup>9</sup>. The TCF4-DN adenovirus was kindly donated by S. J. George (Bristol Heart Institute, Bristol, UK)<sup>10</sup>. Infectious viruses were purified and titered using standard techniques. Briefly, for adenovirus production AD-293T cells were infected with 2 pfu/cell in DMEM without serum for 1 h at 37°C. Then, the infection medium was removed and cells were grown in an appropriate volume of DMEM + 5% horse serum until complete cell lysis was obtained (usually 72h later). The medium containing the viruses was then subjected to 3 freeze-and-thaw cycles in order to destroy all the cells and to free as many virions as possible. The resulting supernatant was then centrifuged at 3000 rpm for 30 min at 4°C to eliminate the cellular debris, aliquoted and stored at -80°C. For the infection of ECs two consecutive cycles of infection [5 h and overnight (O/N)] were performed with MOI of 300 in 1 ml of complete culture medium.

### **Immunofluorescence microscopy**

Immunofluorescence microscopy staining was performed using standard technique, as previously described<sup>11</sup>. Briefly, cells were seeded on 0.5% cross-linked gelatin. Cells were fixed and permeabilized in ice-cold methanol at -20°C for 5 min. Fixed cells were incubated for 30 min in a blocking solution [phosphate buffer saline (PBS) containing Ca<sup>2+</sup> and Mg<sup>2+</sup>, 2.5% skim-milk, 0.3% TritonX-100]. Cells were then incubated for 1 h at RT with primary antibodies diluted in blocking buffer. Alternatively, cells were fixed with 1% PAF in triethanolamine, pH 7.5, containing 0.1% Triton X-100 and 0.1% NP-40 for 20 min. Fixed cells were incubated for 30 min in a blocking solution [Tris-buffered saline (TBS) containing 5% BSA, 0.3% TritonX-100]. Cells were then incubated overnight at 4°C with primary antibodies diluted in blocking buffer. Appropriate secondary antibodies were applied on cells for 45 min at RT and cells were then mounted with VECTASHIELD containing DAPI (Vector Biolabs).

Samples were observed under an epifluorescence microscope (DMR; Leica) using a 63X objective. Images were captured using a charge-coupled camera and processed with Adobe Photoshop. Only adjustments of brightness and contrast were used in the preparation of the figures. For comparison purposes, different sample images of the same antigen were acquired under constant acquisition settings.

### **Western blot analysis**

Total proteins were extracted by solubilising cells in boiling Laemmli buffer [2.5% SDS and 0.125 M Tris-HCl (pH 6.8)]. Lysates were incubated for 5 min at 100°C to allow protein denaturation and then spun for 5 min at 13200 rpm to discard cell debris. The supernatants were collected and the concentration of protein was determined using a BCA™ Protein Assay Kit (Pierce) according to manufacturer's instructions. Equal amounts of proteins were loaded on gel and separated by SDS-PAGE, transferred to a Protran Nitrocellulose Hybridization Transfer Membrane 0.2 µm pore size (Whatman) and blocked for 1 h at RT in 1X TBST Tween (TBST) [150 mM NaCl, 10 mM Tris-HCl (pH 7.4), and 0.05% Tween] containing 5% (w/v) skim-milk. The membranes were incubated overnight at 4°C or 1 h at RT with primary antibodies diluted in 1X TBST-5% BSA. Next, membranes were rinsed 3 times with 1X TBST for 5 min each and incubated for 1 h at RT with HRP-linked secondary antibodies (diluted in 1X TBST-5% BSA). Membranes were rinsed 3 times with TBST for 5 min each and specific binding was detected by the enhanced chemiluminescence (ECL) system (Amersham Biosciences) using Hyperfilm™ (Amersham Biosciences) or the ChemiDoc gel imaging system (BIORAD). The molecular masses of proteins were estimated relatively to the electrophoretic mobility of co-transferred prestained protein marker, Broad Range (Cell Signalling Technology).

### **Co-immunoprecipitation**

Cells were grown until confluent and starved overnight. Cells were then washed once with DMEM without serum and incubated with 0.4 mg/ml of dithiobis(succinimidyl)propionate (DSP) (Pierce) for 30 min at 37°C. After several washes with ice-cold PBS, cells were lysed in ice-cold modified RadioImmunoPrecipitation Assay (RIPA) buffer (Tris HCl pH 7.5 100 mM, NaCl 150 mM, Deoxycholic acid 1%, SDS 0.1%, CaCl<sub>2</sub> 2

mM). The protein lysate was precleared with an appropriate volume of Protein G Sepharose 4B (Zymed) for 3 h at 4°C. Protein concentration was determined with BCA™ Protein Assay Kit and an equal amount of protein was incubated with either immune antibodies or species-matched control antibodies overnight at 4°C. On the following day immunocomplexes were collected using Protein G Sepharose 4B for 3 h at +4°C. Beads were then washed several times with modified RIPA buffer and boiled in an appropriate volume of Laemmli buffer. Samples were analysed by standard Western blot analysis as described above<sup>11</sup>.

CoIP following biotinylation of membrane proteins was performed using the same protocol as above. Before cell lysis with modified RIPA buffer cells were incubated with Sulfo-NHS-LC-Biotin (Pierce ThermoScientific) 0.55 mg/ml in PBS containing Ca<sup>2+</sup> and Mg<sup>2+</sup> pH 8.0 for 30 min at 4°C. After biotinylation cells were washed with PBS containing Ca<sup>2+</sup> and Mg<sup>2+</sup> pH 8.0 + Glycine 100 mM to quench the reaction.

CoIP from lung tissue: lungs from wild type adult age-matched mice were lysed in ice-cold modified JS buffer [Hepes pH 7.5 72 mM, NaCl 210 mM, glycerol 0.5 %, Triton X-100 1%, MgCl<sub>2</sub> 2 mM, EGTA 7.2 mM, SDS 0.1 %, Sodium Orthovanadate 300 mM, Pefabloc SC 1 mM (Sigma) and Sodium Fluoride 1 mM] using Tissue Lyser II (QIAGEN) (two 30-sec pulses at maximum frequency). Samples were precleared for 4 h at 4°C with an appropriate volume of Protein G Sepharose 4B. Protein concentration was determined with BCA™ Protein Assay Kit and an equal amount of protein was incubated with Protein G Sepharose 4B pre-coupled with either immune antibodies or species-matched control antibodies overnight at 4°C. The day after, beads were then washed with modified JS buffer and boiled in an appropriate volume of Laemmli buffer. Samples were analysed by standard western blot analysis<sup>11</sup>. All the buffers contained freshly added protease inhibitor cocktail (IFOM Kitchen Facility).

### **RNA-seq library preparation and sequencing**

1 µg total RNA per sample (in triplicate) was used to prepare RNA sequencing libraries of VEC-null and VEC-positive cells with SMARTer Stranded Total RNA Sample Prep kit - High input Mammalian kit (Clontech), according to the manufacturer's instructions. This kit includes depletion of ribosomal RNA prior to library synthesis, barcoding and amplification. For validation of the amplified RNA-seq library, 1 µl of the library was used with the Agilent High Sensitivity DNA kit (Agilent). The samples were sequenced on a HiSeq2500 sequencing system with v4 chemistry from Illumina at the Swedish National Genomics Infrastructure, Uppsala node, SNP&SEQ technology platform (Science for Life Laboratory, Uppsala). The samples were run in pools of 6 samples with equimolar amounts of dsDNA from each of the six samples. Each pool was run on a single lane (paired-end sequencing, 125bp reads).

### **Bioinformatics analysis of RNA-seq data**

Each sample received ~24 to 46 million of paired-end reads. Trim Galore ([http://www.bioinformatics.babraham.ac.uk/projects/trim\\_galore/](http://www.bioinformatics.babraham.ac.uk/projects/trim_galore/)) was used for quality/adaptor trimming of the raw reads. In addition, 5 nucleotides from both 5' and 3' end of the reads were clipped to remove unwanted bias. Then trimmed reads were mapped to the mm10 mouse genome with > 70% overall mapping rate using TopHat v2.1.1<sup>12</sup> and annotated with GO terms using R package Biomart<sup>13</sup>. Differential gene expression (DEG) analysis was performed using DESeq2<sup>14</sup>. Genes were considered significantly differentially expressed if the  $|\log_2FC| \geq 1$  and the adjusted  $p$ -value  $\leq 0.05$ .

### **Identification of enriched functional annotation categories**

Genes significantly up and downregulated in confluent VEC-positive vs. VEC-null cells were used to query DAVID's<sup>15</sup> "Functional Annotation Clustering" tool to look for enrichment of annotation terms from GOTERM\_BP\_DIRECT, KEGG, BIOCARTA and UP\_KEYWORDS using the *Mus musculus* genome as background. Annotation terms with overlapping gene sets were grouped (see Online Table III for details) and used to annotate an expression heat-map of the same genes across all samples. For the purposes of visualisation abundance is presented as log<sub>2</sub> (normalised read count + 1).

### **Quantitative Real Time (qRT)-PCR analysis**

Total RNA was isolated by RNeasy kit (QIAGEN) and 1 µg was reverse transcribed with random hexamers (High Capacity cDNA Archive Kit, Applied Biosystems) according to the manufacturer's instructions. cDNA (5 ng) was amplified in triplicate in a reaction volume of 15 µl using TaqMan Gene Expression Assay (Applied Biosystems) and an ABI/Prism 7900 HT thermocycler, using a pre-PCR step of 10 min at 95°C, followed by 40 cycles of 15 sec at 95°C and 60 sec at 60°C. Preparations of RNA template without reverse transcriptase were used as negative controls. For any sample the expression level, normalized to the housekeeping gene

18S, glyceraldehyde-3-phosphate dehydrogenase (GAPDH) or  $\beta$ 2-microglobulin, was determined using the comparative threshold cycle (CT) method as previously described<sup>16</sup>.

### Transcription factor binding site analysis

In order to identify FoxO1 and Tcf/ $\beta$ -catenin consensus sequences on the putative *VE-PTP* and *vWf* promoter regions we used the program MatInspector<sup>17</sup>, which identifies transcription factor binding sites (TFBS) in nucleotide sequences using a large library of weight matrices. We analyzed the sequence spanning from 6000 bp upstream and 500 bp downstream the transcription start site (TSS) of the genes and obtained a prediction of a potential combination of TFBS. The TFBS sequences considered in the analysis were [AG][GA][TG][AC]AACAA[AC] for FoxO1 binding and [TAG][GT][AG][CT][AT]x(2)CAAAG[GCT][GAC][AC][GCA] for Tcf/ $\beta$ -catenin binding.

### *Claudin-5* promoter luciferase assay

*Claudin-5* putative promoter region including all three regions of paired Tcf/ $\beta$ -catenin-FoxO1 binding sites<sup>18</sup> (3169 bp upstream of the CDS) was cloned into the XhoI-HindIII site of the multiple cloning region of pGL3-Basic Vector (Promega) using the following primers: 5'-AAAAACTCGAGAAATGGCTCTGGGCAAGAAG-3' and 5'-AGGGAAAGCTTGGCTAAAGACTGAATGCTCA-3'. XhoI and HindIII restriction enzymes were from New England BioLabs. Cloning was confirmed by sequencing, performed by STP Genomics Equipment Park (The Francis Crick Institute, London, UK). VEC-positive cells, wild type or infected with the indicated constructs, were seeded at 30.000 cells/cm<sup>2</sup>; VEC-null cells, wild type or infected with the indicated constructs, were seeded at 55.000 cells/cm<sup>2</sup> in 35 mm diameter plates (Corning) in complete culture medium without penicillin/streptomycin. The day after, cells were transiently transfected with 2  $\mu$ g/well of *Claudin-5*-pGL3-luciferase vector and 1  $\mu$ g/well of pRL-TK vector (Promega) using 8  $\mu$ l/well of LipofectAMINE 2000 (Invitrogen) in OptiMEM (Invitrogen) according to the manufacturer's instructions. After 8.5 h of incubation, cells were incubated in fresh complete culture medium and 72 h after transfection, firefly and Renilla luminescence were detected using Dual-Glo Luciferase Assay System (Promega), according to the manufacturer's instructions, with EnVision 2102 MultiLabel Reader (PerkinElmer). Renilla luminescence signal was used as normalizer for transfection efficiency.

### Protein expression and purification

For GST-tagged VEC-cytoplasmic tail production, bacterial expression vector<sup>19</sup> was transformed into BL21 strain of *E. coli*. For growth, a single colony was picked from freshly transformed plate and allowed to grow overnight at 37°C in 20 ml LB medium. This culture was used to inoculate 2 x 1 liter of LB and TB media. Cultures were allowed to grow until the OD<sub>600nm</sub> reached 0.6 at which point protein expression was induced by the addition of 1 mM IPTG. Induction was allowed to occur at 37°C for 4 h. The cells were then harvested by centrifugation and stored at -80°C until required. Cells obtained from 1 liter of LB or TB media were treated in the same way. Frozen pellets were thawed and resuspended in 20 ml ice cold lysis buffer containing 50 mM HEPES (pH 7.5), 2 mM EDTA, 1 mM DTT and protease inhibitors (Sigma) (2 protease inhibitor tablets were added to 50 ml total lysis buffer). To ensure complete lysis the suspension was sonicated for 5 x 30 sec, 20% amplitude. The insoluble fraction was removed by centrifugation (30,000 rpm, 20 mins, 4°C) and the soluble fraction incubated with 200  $\mu$ l glutathione sepharose for 1 h at 4°C with constant rolling. The resin was then washed extensively with lysis buffer and bound protein eluted using lysis buffer containing 20 mM reduced glutathione. Elutions were concentrated to a volume of 270  $\mu$ l to which 30  $\mu$ l of glycerol was added. The protein concentration was determined by Bradford reagent, snap frozen in liquid nitrogen and stored at -80 °C until required.

For GST-tagged p120-catenin production, competent *E. coli* DH10 Bac cells (Invitrogen) were transformed with GST-Ctnnd1-pFastBAC1 plasmid (NovoPro). White colonies were picked from freshly transformed plates and grown in liquid culture in order to purify bacmid DNA. This DNA was then used to generate virus by transfecting Sf21 insect cells (Invitrogen). Two further rounds of amplification generated high titre virus stocks suitable for infecting large scale cultures for expression of the protein. Sf21 insect cells were infected at a cell density of 1.2 x 10<sup>6</sup> cells/ml and at a MOI of 1. Infected cultures were allowed to grow for 3 days with shaking (140 rpm) at 27°C. Cells were then harvested and cell pellets stored at -80 °C until required. 2L of cell pellet was thawed and resuspended in 30 ml lysis buffer (50 mM HEPES [pH 7.5], 250 mM NaCl, 10% glycerol, 1 % Triton X-100, 1 mM NaF, 10 mM benzamidine, 0.5 mM EDTA, 10 mM B-glycerophosphate, 1 mM Na<sub>2</sub>VO<sub>4</sub>, 1mM DTT) and lysed by sonication on ice (3 min total time, 20 sec on 5 sec off, 20%

amplitude). Insoluble material was removed by centrifugation at 30.000 rpm for 20 mins. The soluble fraction was incubated with 300 µl bed volume of glutathione sepharose resin for 2 h (with rolling at 4°C) after which time the resin was washed extensively in buffer containing 50 mM HEPES (pH7.5), 250 mM NaCl, 1 mM DTT. Protein was eluted in the same wash buffer supplemented with 15 mM reduced glutathione and 5% glycerol.

### **Peptide arrays**

Peptide arrays were synthesised on an Intavis Multiprep Peptide Synthesiser (Intavis Bioanalytical Instruments AG), using N-Fmoc amino acids, onto a cellulose sheet derivitised to have 8-10 ethylene glycol units between the sheet and an amino group for synthesis. Each amino acid was coupled as a chlorohydroxybenzotriazole active ester, automatically formed immediately prior to use. Once the required number of cycles of coupling and deprotection and washing were completed, the membranes were treated with a solution of 20 mls containing 95% trifluoroacetic acid, 3% triisopropylsilane and 2% water for 4 h. Following this treatment, membranes were washed 4 times with dichloromethane, 4 times with ethanol, twice with water, once with ethanol.

Membranes were activated with 100% methanol for 10 seconds and washed twice with 1X TBST (0.1% Tween) for 5 minutes each wash. Membranes were then blocked for 1 h at RT in 1X TBST (0.1% Tween) containing 5% (w/v) skim-milk, and incubated 2 h at RT with free GST (kind gift of S. Tooze, The Francis Crick Institute, London, UK) or GST-tagged VEC-cytoplasmic tail<sup>19</sup>, β-catenin (Sino Biological Inc.) or p120-catenin, diluted to 1 µg/ml in 1X TBST-5% BSA. Next, membranes were rinsed 5 times with 1X TBST (0.1% Tween) and incubated overnight at 4°C with HRP-linked anti-GST antibody (diluted in 1X TBST-5% skim-milk). Membranes were rinsed 5 times with 1X TBST (0.1% Tween) for 5 min each time and specific binding was detected by the enhanced chemiluminescence (ECL) system (Amersham Biosciences) using Hyperfilm<sup>TM</sup> (Amersham Biosciences).

### **Peptide pull-down assays**

Solid phase synthesis of the peptides was carried out on an Intavis Multiprep Peptide Synthesizer (Intavis Bioanalytical Instruments AG) on a Rink amide LL resin, using N-Fmoc amino acids and HCTU as the coupling reagent. In the final steps of chain assembly biotin was incorporated at the N-terminal after an aminohexanoic acid spacer. Following this, the peptidylresin was added to 10 ml of 92.5% trifluoroacetic acid, 2.5% water, 2.5% ethanedithiol and 2.5% triisopropyl silane. After 2 h reaction, the resin was removed by filtration and the peptide was precipitated from the acid solution with diethyl ether on ice. The peptide was isolated by centrifugation, then dissolved in water and freeze dried overnight. After dissolving in water portions of the peptides were purified on a C8 reverse phase HPLC column (Agilent PrepHT Zorbax 300SB-C8, 21.2x250 mm, 7 m). Buffer A was 1% acetonitrile, 0.08% trifluoroacetic acid in water, buffer B was 90% acetonitrile, 0.08% trifluoroacetic acid in water. The elution gradient was from 10% to 50% B over 40 minutes at a flow rate of 8 ml/minute. The peak fraction was analysed by LC-MS on an Agilent 1100 LC-MSD. The calculated molecular weights of the peptide were in agreement with the mass found. For the complete list of peptides used in this study see Online Table IV.

Neutravidin<sup>TM</sup> biotin binding beads (Perbio) were washed 3 times in 1 ml of cold Buffer Y [Tris-HCl pH 7.5 50 mM, NaCl 150 mM, EDTA 1 mM, NP-40 1 % v/v, DTT 1mM, EDTA-free Protease Inhibitor Cocktail (Sigma)] and incubated with the desired biotin-conjugated peptide (1.5 mg/ml in water) at 4°C for 1 h with rotation. Peptide-conjugated beads were washed 3 times in cold Buffer Y and incubated with 2 µg of purified protein in a volume of 500 µl of Buffer Y overnight at 4°C with rotation. Beads were then washed 3 times in Buffer Y and boiled in an appropriate volume of Laemmli buffer. Samples were analysed by standard Western blot analysis as described above.

### **TAT-peptide treatment**

VEC-positive cells were plated at a concentration of 55.000 cells/cm<sup>2</sup> in complete culture medium with 30 µg/ml of TAT-conjugated peptide. Treatment was repeated the following day at the same concentration, followed by 2 other treatments at 10 µg/ml on day 3 and 5. On day 7, after cells had been at confluence for 48 h, cells were starved overnight in starving medium containing 10 µg/ml of TAT-conjugated peptide, then processed for co-immunoprecipitation, ChIP and qRT-PCR.

### **Chromatin immunoprecipitation (ChIP)**

ChIP assays were carried out as previously described<sup>20</sup>. Briefly, cells were starved overnight and cross-linked with 1% PFA for 10 min at RT. PFA was then inactivated by the addition of 125 mM glycine. Cells were then washed and resuspended in lysis buffer. Samples were sonicated with a BIORUPTOR™ 200 using the following conditions: H power, 30 sec ON - 60 sec OFF for 20 min. Chromatin extracts containing from 200 µg to 1000 µg of DNA fragments with an average size of 500 bp were incubated overnight with using 5 µg of either immune antibody or matched non-immune antibodies and Dynabeads protein G (Invitrogen) or Ultralink resin protein A/G (Pierce ThermoScientific). On the following day, beads were recovered and washed twice with Mixed Micelle Wash Buffer (NaCl 150 mM, TrisHCl pH 8.1 20 mM, EDTA 5 mM, Sucrose 5.2 % w/v, NaN<sub>3</sub> 0,02%, Triton X-100 1%, 0.2 % SDS), Buffer 500 (Deoxycholic acid 0,1% w/v, NaCl 500 mM, HEPES pH 7.5 25 mM, EDTA 1 mM, NaN<sub>3</sub> 0.02%, Triton X-100 1%), LiCl Detergent wash (Deoxycholic acid 0,5% w/v, LiCl 250 mM, EDTA 1 mM, NP-40 0.5% v/v, NaN<sub>3</sub> 0.02%, Tris HCl pH 8.0 10 mM). Proteins/DNA complexes were detached from beads by heating the samples at 65°C for 10 min. De-crosslinking was done at 65°C overnight. DNA was purified using phenol/chloroform and precipitated in 70% ethanol according to standard protocol. DNA was amplified by qRT-PCR techniques using oligonucleotides flanking the assayed promoter regions.

Primers used in this experiments were: 5'-GTCGGGTGAGCATTTCAGTCT-3' and 5'-ATCAAGCCCACCCATCCTAC-3' (Claudin-5 TSS); 5'-TGCAGAAGGAGAAAACAATGC-3' and 5'-GCAGCAACGTGTGTCAGTGT-3' (VE-PTP Region 1); 5'-TGGATCCTGTAGCCATATTTGA-3' and 5'-CATCATATAACTGCAACAAAGCAC-3' (VE-PTP Region 2); 5'-GACATAAGTCCAAGAACAGGTTT-3' and 5'-TCAAATCACTAGGAGGAATAAGACA-3' (VE-PTP Region 3); 5'-GCTCAACAAGTGGTACCCAGA-3' and 5'-TGCACGACGCTCAGTGTAT-3' (VE-PTP TSS); 5'-GTTTGTGGTTGAGCCAGGGTCT-3' and 5'-CAGGAGTTCGAAGCAAGATG-3' (vWf Region 1); 5'-GCAGGTCTTGGTTCTATGC-3' and 5'-GGGGTGGAAATGATGGTTC-3' (vWf Region 2); 5'-TGGTGGCAACTTGGAGCTAT-3' and 5'-AGGGGCTTCAAAGTCCTCAG-3' (vWf Region 3/TSS).

For qRT-PCR analyses DNA was diluted in the presence of specific primers (0.4 µM each) to a final volume of 25 µl in SYBR Green Reaction Mix (Perkin Elmer).

### **RNA interference**

Stealth RNAi Duplexes (Life Technologies) and the correspondent Low GC Stealth RNAi Control Duplexes (Life Technologies) were used to knockdown FoxO1. The sequences of the two siRNAs used were the following: 5'-CCAAGUGACUUGGAUGGCAUGUUUA-3' and 5'-CAGACACUUCAGGACAGCAAUCA-3'. Transfection was performed using LipofectAMINE 2000 (Invitrogen) according to the manufacturer's instructions.

### **In vivo pharmacological treatment**

All animal procedures were performed in accordance with the Institutional Animal Care and Use Committee (IACUC), in compliance with the guidelines established in the Principles of Laboratory Animal Care (directive 86/609/EEC) and approved by the Italian Ministry of Health.

Ezh2 and Ezh1 were inhibited in C57Bl/6J background pups by intraperitoneal injection with 50 mg/kg UNC1999<sup>21</sup> in 10% DMSO and 90% corn oil or vehicle only, at P3, P4 and P5. Total RNA from lungs of UNC1999-treated pups (P6) was isolated and processed as described in details previously<sup>22</sup>.

### **Immunohistochemistry (IHC)**

Paraffin-embedded human ovarian tissue samples were scored as pathologic or non-pathologic by a trained pathologist. Samples were de-paraffinized and hydrated following standard protocol and subjected to antigen unmasking in Sodium Citrate Buffer pH 6 for 45 min at 95°C. Samples were stained using MATCH 2 Double Stain 2 Kit (Biocare). Haematoxylin/eosin staining was performed according to standard protocol and samples were mounted in Eukitt (Bio-Optica).

For image quantification we used NIS-Elements AR software (version 4.51.01; Nikon). A hue saturation intensity (HSI) threshold was defined by selecting pixels of specific signal around the vessel perimeter. This threshold was applied to every image, followed by morphometrics steps of image smoothing, cleaning and filling. An area of interest was drawn on images to exclude regions of non-specific staining. Areas of detected specific signal were divided by the total measured surface, and values obtained for Claudin-5 and VE-cadherin were then normalized on the measurements obtained for PECAM1 in the corresponding regions.

## Antibodies and chemicals

Antibodies used in this study were: anti-claudin-5 mouse monoclonal clone 4C3C2, anti-V5 tag mouse monoclonal R960-25 (Life Technologies); anti-claudin-5 rabbit polyclonal ab53765, anti-claudin-5 rabbit monoclonal ab131259, anti-CD31 rabbit polyclonal ab28364, anti-total histone H3 ab1791, anti-H3K4me3 ab8580, and anti-RNA pol II phospho Ser 5 (ABCAM); anti- $\beta$ -catenin mouse monoclonal 610154, anti-Ezh2 mouse monoclonal 612666, anti-N-cadherin mouse monoclonal 610921, anti-Pecam1 rat monoclonal 550274 (BD Biosciences); anti- $\beta$ -catenin rabbit polyclonal 06-734, anti-Ezh2 rabbit polyclonal 07-689, anti-H3K27me3 rabbit polyclonal 07-449, anti-TCF4 mouse monoclonal clone 6H5-3 05-511 (Millipore); anti-FKHR (H-130X) rabbit polyclonal sc-67140, anti-VE-cadherin goat polyclonal sc-6458, anti-vWf clone H-300 rabbit polyclonal sc-14014, anti-Suz12 goat polyclonal sc-46264 (Santa Cruz Biotechnology); anti-vWf rabbit polyclonal AB7356 (Chemicon); anti-FoxO1 rabbit monoclonal clone C29H4 2880, anti-phospho-FoxO1 (Ser 256) rabbit polyclonal 9461, anti-Myc-tag rabbit polyclonal 2272, anti-Suz12 rabbit monoclonal D39F6 3737, anti-H3K27me3 clone C36B11 rabbit monoclonal BK9733BFS, anti- $\beta$ -catenin rabbit monoclonal 8480S (Cell Signalling), anti-Ezh2 mouse monoclonal NCL-L-EZH2 (Novocastra-Leica), peroxidase-conjugated streptavidin (Jackson ImmunoResearch Laboratories), anti-HA-tag mouse monoclonal clone 12CA5, anti-Bmi1 mouse monoclonal clone AF27 [from K. Helin, Biotech research and Innovation Centre (BRIC), University of Copenhagen], anti-Ezh2 clone AC22 and AE25-13, anti- $\alpha$ -tubulin mouse monoclonal, anti-vinculin mouse monoclonal (from internal service); anti-human VE-cadherin mouse monoclonal (BV9)<sup>23</sup>, anti-VE-PTP Rabbit polyclonal (produced in our laboratory), anti-human VE-PTP Rabbit Polyclonal hPTP1-8 from D. Vestweber<sup>24</sup>; HRP-linked anti-GST RPN1236 (GE/Amersham); anti-VE-cadherin rabbit polyclonal 36-1900 (ThermoFisher); anti-Ezh2 rabbit polyclonal 21800-1-AP (Proteintech). The following reagents were used in this study: pan-caspase inhibitor Z-VAD-FMK (Promega); PI3K inhibitor LY294002 (Cell Signalling Technology). To inhibit PI3K activity, cells were starved for 24h in starving medium + 1% BSA and then treated overnight with LY294002 10  $\mu$ M or Dimethyl sulfoxide (DMSO) as a control. To avoid apoptotic cell death during FKHR-TM overexpression experiments, 24h after the beginning of the infection, cells were treated with Z-VAD-FMK 50  $\mu$ M.

## Statistical analysis

Student's two-tailed unpaired t-test was used to determine statistical significance. The significance level was set at  $P < 0.05$ .

## ONLINE FIGURE LEGENDS

### Online Figure I. VEC clustering induces *VE-PTP* and *vWf* expression through FoxO1/ $\beta$ -catenin inhibition.

(A) qRT-PCR and WB analysis of *VE-PTP* and *vWf* expression in sparse (sp) and confluent (con) VEC-null and VEC-positive ECs (upper panel). Immunofluorescence analysis of VEC (green) and *VE-PTP* or *vWf* expression (red) in confluent VEC-null and VEC-positive ECs. Scale bar: 10  $\mu$ m (lower panel).

(B) qRT-PCR analysis of *VE-PTP* and *vWf* expression in VEC-null and VEC-positive ECs expressing FKHR-TM or GFP as a negative control. To limit the pro-apoptotic effect of FKHR-TM, after adenoviral infection the pan-caspase inhibitor Z-VAD-FMK (50  $\mu$ M) was added to culture medium. qRT-PCR was performed 72 h after infection. The levels of mRNA are normalized to Glyceraldehyde-3-Phosphate Dehydrogenase (*GAPDH*), columns are means  $\pm$  s.e.m. of triplicates from a typical experiment. nd, not detectable.

(C) qRT-PCR analysis of *VE-PTP* and *vWf* expression in confluent VEC-null and VEC-positive ECs treated with the PI3K inhibitor LY294002 (10  $\mu$ M, overnight). Upper panel: WB analysis of p-FoxO1 Ser 256 (arrow) and total FoxO1 protein.

(D) qRT-PCR analysis of *VE-PTP* and *vWf* expression in confluent VEC-null and VEC-positive cells expressing  $\Delta$ N- $\beta$ -catenin or GFP as negative control.

(E) Schematic representation of the putative promoter regions of *VE-PTP* and *vWf*. FoxO1 (F) binding sites are depicted as white boxes and TCF/ $\beta$  catenin (T) binding sites as black boxes. Arrows identify primers used for qChIP shown in panels F and G.

(F) qRT-PCR for Region 1, 2 and 3 of *VE-PTP* and *vWf* promoter regions performed on endogenous FoxO1-bound chromatin immunoprecipitated from confluent VEC-null and VEC-positive ECs.

(G) qRT-PCR for Region 1, 2 and 3 of *VE-PTP* and *vWf* promoter regions performed on endogenous  $\beta$ -catenin-bound chromatin immunoprecipitated from confluent VEC-null and VEC-positive ECs.

In (A) and (C) vinculin was used as loading control.

In (A), (C) and (D) the levels of mRNA are normalized to 18S; columns are means  $\pm$  s.e.m. of triplicates from a representative experiment.

In (B), (C) and (D)  $**P < 0.01$ , *t*-test.

In (F) and (G) the levels of DNA are normalized to input, columns are means  $\pm$  st.dev. of triplicates from a representative experiment. nd, not detectable.  $*P < 0.05$ ;  $**P < 0.01$ , *t*-test VEC-null vs. VEC-positive.

#### **Online Figure II. Validation of RNA-seq results.**

(A) qRT-PCR analysis of *Tiam1*, *Lmo2*, *Stat6* and *Elk3* expression in confluent VEC-null and VEC-positive ECs.

(B) qRT-PCR analysis of *Hey1* and *Adm* expression in confluent VEC-null and VEC-positive ECs.

(C) qRT-PCR analysis of *Pecam1* and *Sox18* expression in confluent VEC-null and VEC-positive ECs.

(D) qRT-PCR analysis of *Claudin-5*, *VE-PTP* and *VWF* expression in sparse (sp) and confluent (con) HMEC1.

(E) qRT-PCR analysis of *TIAM1*, *LMO2*, *STAT6* and *ELK3* expression in sparse (sp) and confluent (con) HMEC1.

(F) qRT-PCR analysis of *HEY1* and *ADM* expression in sparse (sp) and confluent (con) HMEC1.

(G) qRT-PCR analysis of *PECAM1* and *SOX18* expression in sparse (sp) and confluent (con) HMEC1.

In the figure, the levels of mRNA are normalized to *GAPDH*; columns are means  $\pm$  s.e.m. of triplicates from a representative experiment.  $*P < 0.05$ ;  $**P < 0.01$ , *t*-test.

#### **Online Figure III. *VE-PTP* and *vWf* genes are repressed in IL2-VEC ECs.**

qRT-PCR analysis of *VE-PTP* and *vWf* expression in confluent VEC-null, VEC-positive and IL2-VEC ECs. The levels of mRNA are normalized to 18S; columns are means  $\pm$  s.e.m. of triplicates from a representative experiment.  $*P < 0.01$ , *t*-test.

#### **Online Figure IV. Histone density on the TSS of *claudin-5*, *VE-PTP* and *vWf* is not affected by VEC expression.**

qRT-PCR for the TSS of *claudin-5*, *VE-PTP* and *vWf* performed on endogenous histone H3-bound chromatin immunoprecipitated from confluent VEC-null and VEC-positive ECs. The levels of DNA are normalized to input, columns are means  $\pm$  st.dev. of triplicates from a representative experiment.

#### **Online Figure V. *Claudin-5* luciferase reporter assays.**

(A) Schematic representation of the putative promoter region of *claudin-5* cloned upstream of firefly luciferase gene. FoxO1 (F) binding sites are depicted as white boxes and TCF/ $\beta$  catenin (T) binding sites as black boxes.

(B) *Claudin-5* luciferase reporter assay performed on confluent VEC-null and VEC-positive cells.

(C) *Claudin-5* luciferase reporter assay performed on confluent VEC-positive ECs upon Suz12 overexpression.

(D) *Claudin-5* luciferase reporter assay performed on confluent VEC-null ECs upon Suz12 knockdown (sh-Suz12).

In (B), (C) and (D)  $*P < 0.05$ ;  $**P < 0.01$ , *t*-test.

#### **Online Figure VI. Effect of Suz12 overexpression on endothelial genes.**

(A) qRT-PCR analysis of *Lmo2* and *Stat6* expression in confluent VEC-positive ECs upon Suz12 overexpression.

(B) qRT-PCR analysis of *Hey1* expression in confluent VEC-positive ECs upon Suz12 overexpression.

(C) qRT-PCR analysis of *Pecam1* and *Sox18* expression in confluent VEC-positive ECs upon Suz12 overexpression.

In the figure, the levels of mRNA are normalized to *GAPDH*; columns are means  $\pm$  s.e.m. of triplicates from a representative experiment.  $*P < 0.05$ ;  $**P < 0.01$ , *t*-test.

#### **Online Figure VII. FoxO1 mRNA levels are unaltered upon stable PcG protein knockdown.**

qRT-PCR analysis of *FoxO1* expression in confluent VEC-null sh-Empty and VEC-null sh-Suz12 ECs. The levels of mRNA are normalized to 18S; columns are means  $\pm$  s.e.m. of triplicates from a representative experiment.

**Online Figure VIII. FoxO1 and Suz12 cooperate for repressing *claudin-5* expression.**

(A) WB analysis of FKHR-TM, Suz12, H3K27me3 and *claudin-5* in extracts of confluent VEC-null, VEC-positive-Empty and VEC-positive-Suz12 ECs expressing FKHR-TM or GFP (negative control). Tubulin is the loading control.

(B) qRT-PCR analysis of *claudin-5* expression in VEC-null, VEC-positive-Empty and VEC-positive-Suz12 ECs expressing FKHR-TM or GFP (negative control). Levels of mRNA are normalized to GAPDH. Columns are means  $\pm$  s.e.m. of triplicates from a representative experiment. \* $P < 0.01$ , t-test.

**Online Figure IX. Ezh2 peptide arrays.**

Peptide arrays with overlapping 20-mers spanning the whole sequence of murine Ezh2 spotted on membrane, probed with indicated GST-tagged proteins in (B), (C) and (D) or free GST as control (A), and analysed by WB. Red dots identify peptides selected for streptavidin pull-down experiments shown in Figure 6. Green boxes define the areas shown in Figure 6B, 6F and 6L.

**Online Figure X. Ezh2 interacts with p120-catenin.**

Co-immunoprecipitation and WB of endogenous Ezh2 and p120-catenin from extracts of confluent VEC-null and VEC-positive ECs.

**Online Figure XI. VE-PTP downregulation in vessels of serous surface papillary ovarian carcinoma.**

IHC staining of VE-PTP expression in sections of human healthy ovary (left panel) or serous surface papillary ovarian carcinoma (right panel). Black arrowheads point to tumor vessel ECs expressing high levels of EZH2. Scale bar: 40  $\mu$ m.

## ONLINE TABLES

### Online Table I. Significantly upregulated endothelial genes in VEC-positive vs VEC-null ECs.

Complete list of endothelial genes significantly upregulated in VEC-positive cells according to the threshold  $|\log_2FC| \geq 1$  and adjusted p-value (padj)  $\leq 0.05$ . List refers to Figure 1B.

| Ensembl_gene_id    | External_gene_name | log2FoldChange | padj        |
|--------------------|--------------------|----------------|-------------|
| ENSMUSG00000021458 | 2010111101Rik      | 1.030144555    | 0.000155219 |
| ENSMUSG00000020681 | Ace                | 1.080455751    | 2.39E-08    |
| ENSMUSG00000054808 | Actn4              | 1.571394864    | 5.72E-85    |
| ENSMUSG00000000530 | Acvrl1             | 3.011281082    | 3.07E-116   |
| ENSMUSG00000022893 | Adamts1            | 1.207992156    | 3.01E-34    |
| ENSMUSG00000069833 | Ahnak              | 1.002778723    | 4.12E-19    |
| ENSMUSG00000019256 | Ahr                | 2.306899238    | 8.88E-74    |
| ENSMUSG00000066406 | Akap13             | 1.147082083    | 3.31E-30    |
| ENSMUSG00000021895 | Arhgef3            | 1.557740572    | 2.19E-62    |
| ENSMUSG00000055116 | Arntl              | 1.63486021     | 1.38E-11    |
| ENSMUSG00000051669 | AU021092           | 2.631170051    | 4.87E-77    |
| ENSMUSG00000037458 | Azin1              | 1.694521168    | 9.20E-37    |
| ENSMUSG00000049792 | Bag5               | 1.037512828    | 5.20E-14    |
| ENSMUSG00000059588 | Calcr1             | 2.353845544    | 1.21E-91    |
| ENSMUSG00000007655 | Cav1               | 1.227512235    | 2.91E-32    |
| ENSMUSG00000000058 | Cav2               | 1.463840099    | 1.96E-19    |
| ENSMUSG00000022661 | Cd200              | 1.565319838    | 2.62E-12    |
| ENSMUSG00000033502 | Cdc14a             | 1.780455692    | 9.75E-33    |
| ENSMUSG00000036533 | Cdc42ep3           | 2.127347302    | 4.40E-35    |
| ENSMUSG00000023067 | Cdkn1a             | 1.582084046    | 2.75E-12    |
| ENSMUSG00000071637 | Cebpd              | 1.007602909    | 0.011257482 |
| ENSMUSG00000041378 | Cldn5              | 5.617650065    | 5.83E-76    |
| ENSMUSG00000023959 | Clic5              | 1.947174651    | 8.18E-105   |
| ENSMUSG00000003617 | Cp                 | 3.425553469    | 3.73E-39    |
| ENSMUSG00000006360 | Crip1              | 4.100612414    | 8.93E-20    |
| ENSMUSG00000061353 | Cxcl12             | 1.61906941     | 4.58E-11    |
| ENSMUSG00000028195 | Cyr61              | 1.614984821    | 1.58E-10    |
| ENSMUSG00000022150 | Dab2               | 1.108024746    | 5.42E-21    |
| ENSMUSG00000002257 | Def6               | 2.77107749     | 1.67E-11    |
| ENSMUSG00000040631 | Dok4               | 1.004119184    | 1.66E-14    |
| ENSMUSG00000003518 | Dusp3              | 1.335031683    | 3.23E-57    |
| ENSMUSG00000028108 | Ecm1               | 1.087583892    | 2.06E-12    |
| ENSMUSG00000008398 | Elk3               | 1.080804982    | 2.57E-37    |
| ENSMUSG00000022505 | Emp2               | 1.577772246    | 8.46E-12    |
| ENSMUSG00000024140 | Epas1              | 1.005688736    | 1.04E-33    |
| ENSMUSG00000038776 | Ephx1              | 1.351199263    | 1.93E-14    |
| ENSMUSG00000024778 | Fas                | 4.169362351    | 4.39E-36    |
| ENSMUSG00000003420 | Fcgrt              | 1.978980212    | 6.33E-51    |
| ENSMUSG00000040170 | Fmo2               | 2.04526583     | 0.000500035 |

|                    |         |             |             |
|--------------------|---------|-------------|-------------|
| ENSMUSG0000009687  | Fxyd5   | 1.339637934 | 8.36E-24    |
| ENSMUSG00000015312 | Gadd45b | 1.483447133 | 0.000612635 |
| ENSMUSG00000034201 | Gas2l1  | 1.006587513 | 1.30E-09    |
| ENSMUSG00000021360 | Gcnt2   | 1.904024924 | 2.17E-15    |
| ENSMUSG00000055737 | Ghr     | 1.411347191 | 3.38E-16    |
| ENSMUSG00000054435 | Gimap4  | 2.783636744 | 4.28E-105   |
| ENSMUSG00000050105 | Grrp1   | 1.129108898 | 0.025674785 |
| ENSMUSG00000040562 | Gstm2   | 2.083053527 | 1.45E-12    |
| ENSMUSG00000067212 | H2-T23  | 1.48958506  | 3.67E-20    |
| ENSMUSG00000071379 | Hpcal1  | 1.160288402 | 4.98E-09    |
| ENSMUSG00000003541 | Ier3    | 2.349737755 | 2.52E-10    |
| ENSMUSG00000074896 | Ifit3   | 1.814510316 | 3.07E-15    |
| ENSMUSG00000005533 | Igflr   | 1.840922626 | 0.000836188 |
| ENSMUSG00000022969 | Il10rb  | 1.029032008 | 4.36E-10    |
| ENSMUSG00000017057 | Il13ra1 | 1.234914814 | 0.036664413 |
| ENSMUSG00000018899 | Irf1    | 1.203207384 | 6.74E-14    |
| ENSMUSG00000027276 | Jag1    | 1.101653799 | 6.97E-17    |
| ENSMUSG00000021294 | Kif26a  | 1.432481827 | 1.15E-15    |
| ENSMUSG00000031788 | Kifc3   | 1.976925202 | 9.04E-28    |
| ENSMUSG00000055148 | Klf2    | 1.488630726 | 1.41E-18    |
| ENSMUSG00000003032 | Klf4    | 2.801834854 | 6.83E-94    |
| ENSMUSG00000033863 | Klf9    | 2.562506604 | 2.76E-36    |
| ENSMUSG00000021959 | Lats2   | 1.193141326 | 5.64E-25    |
| ENSMUSG00000054263 | Lifr    | 1.084566843 | 2.40E-06    |
| ENSMUSG00000032698 | Lmo2    | 1.511260593 | 5.22E-37    |
| ENSMUSG00000016520 | Lnx2    | 1.290227959 | 1.83E-20    |
| ENSMUSG00000068015 | Lrch1   | 1.419034427 | 7.97E-37    |
| ENSMUSG00000040488 | Ltbp4   | 1.12334367  | 8.90E-07    |
| ENSMUSG00000001089 | Luzp1   | 1.028630163 | 5.55E-19    |
| ENSMUSG00000075602 | Ly6a    | 1.812932107 | 1.17E-16    |
| ENSMUSG00000022587 | Ly6e    | 1.028516047 | 2.27E-11    |
| ENSMUSG00000042622 | Maff    | 1.194577554 | 0.017765841 |
| ENSMUSG00000028862 | Map3k6  | 1.348510986 | 0.038153326 |
| ENSMUSG00000001493 | Meox1   | 4.746823504 | 1.38E-22    |
| ENSMUSG00000022353 | Mtss1   | 1.425709869 | 1.67E-56    |
| ENSMUSG00000037235 | Mxd4    | 1.105213479 | 3.24E-35    |
| ENSMUSG00000021365 | Nedd9   | 1.012790987 | 7.52E-23    |
| ENSMUSG00000003847 | Nfat5   | 1.085110516 | 2.67E-30    |
| ENSMUSG00000021025 | Nfkbia  | 1.26736757  | 5.21E-09    |
| ENSMUSG00000021806 | Nid2    | 2.24487386  | 1.32E-126   |
| ENSMUSG00000020889 | Nr1d1   | 2.192153131 | 2.56E-11    |
| ENSMUSG00000020019 | Ntn4    | 1.060251028 | 2.58E-13    |
| ENSMUSG00000022146 | Osmr    | 2.214586778 | 5.94E-05    |
| ENSMUSG00000024725 | Ostf1   | 1.483312676 | 2.43E-32    |
| ENSMUSG00000024805 | Pcgf5   | 1.427740658 | 0.000138545 |
| ENSMUSG00000051177 | Plcb1   | 2.625979803 | 3.78E-89    |

|                    |           |             |             |
|--------------------|-----------|-------------|-------------|
| ENSMUSG00000032377 | Plscr4    | 2.938641363 | 1.61E-09    |
| ENSMUSG00000017754 | Pltp      | 3.603782243 | 4.70E-44    |
| ENSMUSG00000047714 | Ppp1r2    | 1.133018396 | 2.00E-41    |
| ENSMUSG00000053198 | Prx       | 1.312060881 | 4.93E-07    |
| ENSMUSG00000027864 | Ptgfrn    | 1.760648665 | 0.001114651 |
| ENSMUSG00000059895 | Ptp4a3    | 1.076091502 | 4.20E-14    |
| ENSMUSG00000020154 | Ptprb     | 1.870491603 | 2.59E-102   |
| ENSMUSG00000020151 | Ptprr     | 3.906271548 | 1.03E-14    |
| ENSMUSG00000009291 | Pttglip   | 1.494446887 | 6.28E-54    |
| ENSMUSG00000062232 | Rapgef2   | 1.384227356 | 1.15E-36    |
| ENSMUSG00000054364 | Rhob      | 1.181079153 | 3.54E-19    |
| ENSMUSG00000033107 | Rnfl25    | 1.575761287 | 1.32E-12    |
| ENSMUSG00000021067 | Sav1      | 1.563868928 | 3.56E-41    |
| ENSMUSG00000028780 | Sema3c    | 1.166899613 | 0.006795405 |
| ENSMUSG00000071178 | Serpina1b | 4.035515589 | 4.23E-19    |
| ENSMUSG00000071177 | Serpina1d | 3.738797408 | 3.27E-13    |
| ENSMUSG00000072849 | Serpina1e | 3.335872183 | 3.95E-10    |
| ENSMUSG00000017756 | Slc12a7   | 2.252879677 | 5.02E-69    |
| ENSMUSG00000037434 | Slc30a1   | 1.178611424 | 2.16E-21    |
| ENSMUSG00000025993 | Slc40a1   | 1.018321315 | 5.11E-10    |
| ENSMUSG00000030096 | Slc6a6    | 1.770344183 | 2.31E-17    |
| ENSMUSG00000002504 | Slc9a3r2  | 1.286876353 | 7.09E-34    |
| ENSMUSG00000032548 | Slco2a1   | 2.471737479 | 6.58E-10    |
| ENSMUSG00000025006 | Sorbs1    | 1.153251032 | 5.20E-14    |
| ENSMUSG00000031626 | Sorbs2    | 1.075504026 | 3.75E-14    |
| ENSMUSG00000002147 | Stat6     | 1.511251856 | 4.96E-28    |
| ENSMUSG00000014813 | Stc1      | 1.078916739 | 8.98E-40    |
| ENSMUSG00000039156 | Stim2     | 1.240683389 | 1.07E-45    |
| ENSMUSG00000030711 | Sult1a1   | 1.055824496 | 0.014286389 |
| ENSMUSG00000096054 | Syne1     | 1.043358879 | 1.65E-14    |
| ENSMUSG00000038213 | Tapbpl    | 1.210269439 | 3.14E-06    |
| ENSMUSG00000006642 | Tcf23     | 2.402352937 | 1.27E-08    |
| ENSMUSG00000020034 | Tcp1l12   | 1.137117364 | 1.82E-08    |
| ENSMUSG00000002489 | Tiam1     | 2.185948789 | 4.27E-102   |
| ENSMUSG00000020044 | Timp3     | 1.710305929 | 9.82E-89    |
| ENSMUSG00000034640 | Tiparp    | 3.307295131 | 3.95E-127   |
| ENSMUSG00000020023 | Tmcc3     | 2.227468759 | 9.42E-09    |
| ENSMUSG00000037573 | Tob1      | 1.334672963 | 6.87E-13    |
| ENSMUSG00000020601 | Trib2     | 1.368183264 | 4.98E-15    |
| ENSMUSG00000047821 | Trim16    | 1.05040397  | 5.32E-08    |
| ENSMUSG00000020773 | Trim47    | 1.808934868 | 3.01E-18    |
| ENSMUSG00000042116 | Vwa1      | 4.388395603 | 7.03E-88    |
| ENSMUSG00000001930 | Vwf       | 2.10472827  | 3.69E-88    |
| ENSMUSG00000044786 | Zfp36     | 1.277531768 | 0.007208359 |
| ENSMUSG00000041703 | Zic5      | 1.557135924 | 0.011888894 |

**Online Table II. Significantly downregulated endothelial genes in VEC-positive vs VEC-null ECs.**

Complete list of endothelial genes significantly downregulated in VEC-positive cells according to the threshold  $|\log_2FC| \geq 1$  and adjusted p-value (padj)  $\leq 0.05$ . List refers to Figure 1B.

| Ensembl_gene_id    | External_gene_name | log2FoldChange | padj        |
|--------------------|--------------------|----------------|-------------|
| ENSMUSG00000025085 | Ablim1             | -1.945664238   | 5.37E-24    |
| ENSMUSG00000026003 | Acadl              | -1.086609504   | 2.58E-10    |
| ENSMUSG00000030790 | Adm                | -1.608017282   | 0.010413999 |
| ENSMUSG00000038587 | Akap12             | -1.726967454   | 2.61E-34    |
| ENSMUSG00000041688 | Amot               | -1.758695706   | 2.43E-32    |
| ENSMUSG00000071847 | Apcdd1             | -1.149995659   | 0.001802338 |
| ENSMUSG00000027792 | Bche               | -1.514352417   | 0.013541964 |
| ENSMUSG00000026278 | Bok                | -1.289180293   | 0.000255985 |
| ENSMUSG00000026029 | Casp8              | -1.067999624   | 2.80E-19    |
| ENSMUSG00000041598 | Cdc42ep4           | -1.048941056   | 0.008913035 |
| ENSMUSG00000037664 | Cdkn1c             | -1.557952614   | 4.96E-06    |
| ENSMUSG00000052560 | Cpne8              | -2.080693021   | 6.82E-28    |
| ENSMUSG00000044258 | Ctla2a             | -1.245822534   | 7.41E-19    |
| ENSMUSG00000074874 | Ctla2b             | -1.670778565   | 6.31E-25    |
| ENSMUSG00000019891 | Dcbld1             | -1.138077823   | 0.004201829 |
| ENSMUSG00000057098 | Ebf1               | -2.111413582   | 9.99E-12    |
| ENSMUSG00000027954 | Efna1              | -1.200342638   | 1.03E-18    |
| ENSMUSG00000041773 | Enc1               | -1.79080039    | 1.66E-23    |
| ENSMUSG00000043556 | Fbxl7              | -3.775920835   | 5.86E-14    |
| ENSMUSG00000038372 | Gmcs               | -1.004691345   | 0.004715295 |
| ENSMUSG00000056870 | Gulp1              | -1.419817989   | 0.020827657 |
| ENSMUSG00000040289 | Hey1               | -2.020566228   | 6.67E-08    |
| ENSMUSG00000007872 | Id3                | -1.394713645   | 2.94E-07    |
| ENSMUSG00000026896 | Ifih1              | -1.325927571   | 0.010695402 |
| ENSMUSG00000078853 | Igtp               | -1.198266255   | 0.020467277 |
| ENSMUSG00000031304 | Il2rg              | -3.162676661   | 2.01E-14    |
| ENSMUSG00000031734 | Irx3               | -2.38750018    | 6.26E-20    |
| ENSMUSG00000031239 | Itm2a              | -1.759963614   | 4.14E-06    |
| ENSMUSG00000098557 | Kctd12             | -1.851946008   | 1.84E-06    |
| ENSMUSG00000057722 | Lepr               | -1.490989244   | 0.005647257 |
| ENSMUSG00000018169 | Mfng               | -2.644030792   | 9.44E-15    |
| ENSMUSG00000023094 | Msr2               | -1.333390874   | 0.000634309 |
| ENSMUSG00000020900 | Myh10              | -1.492692468   | 1.59E-35    |
| ENSMUSG00000018417 | Myo1b              | -3.305487303   | 1.90E-133   |
| ENSMUSG00000046949 | Nqo2               | -1.085224089   | 1.64E-09    |
| ENSMUSG00000033377 | Palmd              | -1.624208436   | 0.004043486 |
| ENSMUSG00000031379 | Pir                | -4.724267197   | 1.95E-22    |
| ENSMUSG00000042842 | Serp1b6            | -1.942757029   | 1.63E-06    |
| ENSMUSG00000045629 | Sh3tc2             | -6.052872043   | 1.87E-43    |
| ENSMUSG00000040710 | St8sia4            | -2.233886401   | 7.77E-46    |
| ENSMUSG00000037820 | Tgm2               | -5.967240498   | 4.34E-191   |

|                    |          |              |          |
|--------------------|----------|--------------|----------|
| ENSMUSG00000060548 | Tnfrsf19 | -1.869105773 | 2.51E-11 |
| ENSMUSG00000020577 | Tspan13  | -5.490186323 | 1.60E-39 |
| ENSMUSG00000001473 | Tubb6    | -1.290729983 | 4.37E-30 |

**Online Table III. Grouping of functional annotation categories.**

Explanation of how different annotation terms with overlapping gene sets were grouped in Figure 1C graphical representation.

| Direction | Group  | Group in Figure 1C                                      |
|-----------|--|---|
| down      | UP_KEYWORDS: Cell cycle  | cell cycle  |
| down      | GOTERM_BP_DIRECT: GO:0007049~cell cycle  | cell cycle  |
| down      | UP_KEYWORDS: Cytoskeleton  | cytoskeleton  |
| down      | UP_KEYWORDS: Phosphoprotein  | phosphoprotein / signal                                 |
| down      | GOTERM_BP_DIRECT: GO:0007052~mitotic spindle organization                          | mitotic spindle organization                            |
| down      | UP_KEYWORDS: Cell projection   | cell projection   |
| down      | UP_KEYWORDS: Cyclin  | cell proliferation / cyclin                             |
| down      | GOTERM_BP_DIRECT: GO:0008283~cell proliferation                                    | cell proliferation / cyclin                             |
| down      | GOTERM_BP_DIRECT: GO:0002040~sprouting angiogenesis                                | sprouting angiogenesis                                  |
| up        | UP_KEYWORDS: Glycoprotein  | glycoprotein  |
| up        | UP_KEYWORDS: Disulfide bond  | disulfide bond  |
| up        | UP_KEYWORDS: Signal  | phosphoprotein / signal                                 |
| up        | KEGG_PATHWAY: mmu04510:Focal adhesion  | ECM-receptor interaction / focal adhesion               |
| up        | KEGG_PATHWAY: mmu04151:PI3K-Akt signaling pathway                                  | PI3K-AKT signaling pathway                              |
| up        | KEGG_PATHWAY: mmu04512:ECM-receptor interaction                                    | ECM-receptor interaction / focal adhesion               |
| up        | UP_KEYWORDS: Developmental protein   | developmental protein / differentiation                 |
| up        | UP_KEYWORDS: Differentiation   | developmental protein / differentiation                 |
| up        | UP_KEYWORDS: Membrane  | membrane / transmembrane                                |
| up        | UP_KEYWORDS: Transmembrane   | membrane / transmembrane                                |
| up        | UP_KEYWORDS: Protein phosphatase   | protein phosphatase / transferase                       |
| up        | UP_KEYWORDS: Kinase  | kinase  |
| up        | UP_KEYWORDS: Transferase   | protein phosphatase / transferase                       |
| up        | UP_KEYWORDS: Serine/threonine-protein kinase                                       | kinase  |
| up        | BIOCARTA: m_raccycdPathway:Influence of Ras and Rho proteins on G1 to S Transition | influence of Ras and Rho proteins on G1 to S transition |
| up        | UP_KEYWORDS: Cell cycle  | cell cycle  |

**Online Table IV. Complete list of peptides used in this study.**

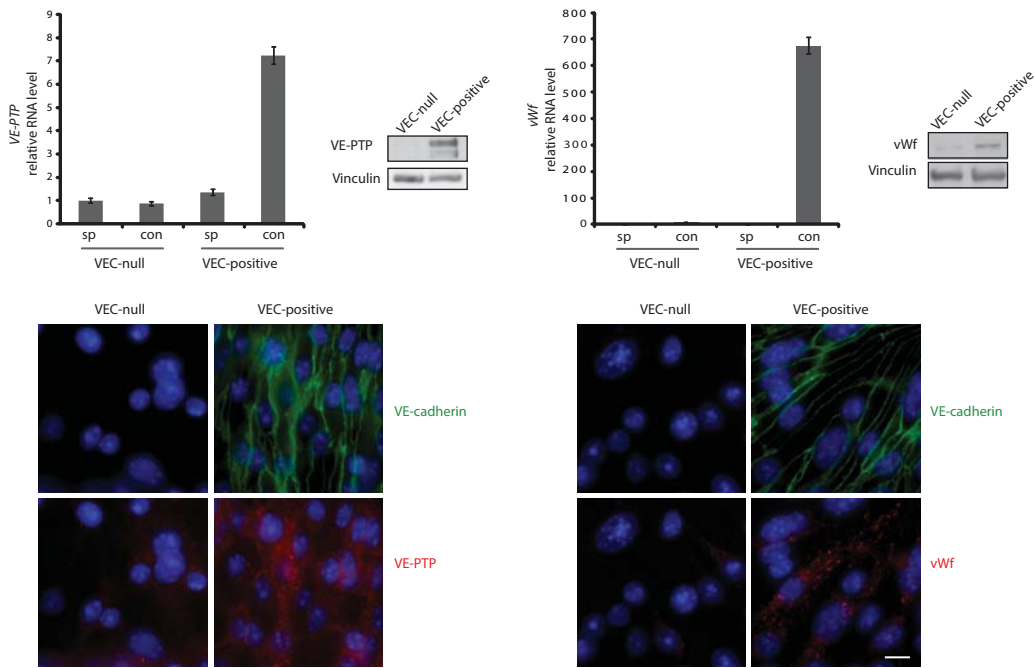
| Biotinylated peptides used in pull-down assays |   |
|--|---|
| A2   | Biotin-X-G-Q-T-G-K-K-S-E-K-G-P-V-C-W-R-K-R-V-K-S-CONH2              |
| A18  | Biotin-X-R-V-K-S-E-Y-M-R-L-R-Q-L-K-R-F-R-R-A-D-E-CONH2              |
| B33  | Biotin-X-I-M-T-S-V-S-S-L-R-G-T-R-E-C-S-V-T-S-D-L-CONH2              |
| C2   | Biotin-X-S-L-R-G-T-R-E-C-S-V-T-S-D-L-D-F-P-A-Q-V-CONH2              |
| E12  | Biotin-X-D-R-E-C-G-F-I-N-D-E-I-F-V-E-L-V-N-A-L-G-CONH2              |
| F10  | Biotin-X-E-R-E-E-K-Q-K-D-L-E-D-N-R-D-D-K-E-T-C-P-CONH2              |
| H34  | Biotin-X-D-C-F-L-H-P-F-H-A-T-P-N-T-Y-K-R-K-N-T-E-CONH2              |
| I9   | Biotin-X-T-Y-K-R-K-N-T-E-T-A-L-D-N-K-P-C-G-P-Q-C-CONH2              |
| I27  | Biotin-X-Q-C-Y-Q-H-L-E-G-A-K-E-F-A-A-A-L-T-A-E-R-CONH2              |
| K31  | Biotin-X-K-D-E-T-S-S-S-E-A-N-S-R-C-Q-T-P-I-K-M-CONH2                |
| K35  | Biotin-X-S-S-S-E-A-N-S-R-C-Q-T-P-I-K-M-K-P-N-I-CONH2                |
| L4   | Biotin-X-N-S-R-C-Q-T-P-I-K-M-K-P-N-I-E-P-P-E-N-V-CONH2              |
| L5   | Biotin-X-S-R-C-Q-T-P-I-K-M-K-P-N-I-E-P-P-E-N-V-E-CONH2              |
| L7   | Biotin-X-C-Q-T-P-I-K-M-K-P-N-I-E-P-P-E-N-V-E-W-S-CONH2              |
| M6   | Biotin-X-N-F-C-A-I-A-R-L-I-G-T-K-T-C-R-Q-V-Y-E-F-CONH2              |
| M10  | Biotin-X-I-A-R-L-I-G-T-K-T-C-R-Q-V-Y-E-F-R-V-K-E-CONH2              |
| M17  | Biotin-X-K-T-C-R-Q-V-Y-E-F-R-V-K-E-S-I-I-A-P-V-CONH2                |
| M26  | Biotin-X-R-V-K-E-S-S-I-I-A-P-V-P-T-E-D-V-D-T-P-P-CONH2              |
| N3   | Biotin-X-D-V-D-T-P-P-R-K-K-K-R-K-H-R-L-W-A-A-H-C-CONH2              |
| N22  | Biotin-X-C-R-K-I-Q-L-K-K-D-G-S-S-N-H-V-Y-N-Y-Q-P-CONH2              |
| N35  | Biotin-X-H-V-Y-N-Y-Q-P-C-D-H-P-R-Q-P-C-D-S-S-C-P-CONH2              |
| O4   | Biotin-X-P-C-D-H-P-R-Q-P-C-D-S-S-C-P-C-V-I-A-Q-N-CONH2              |
| O25  | Biotin-X-C-E-K-F-C-Q-C-S-S-E-C-Q-N-R-F-P-G-C-R-C-CONH2              |
| O28  | Biotin-X-F-C-Q-C-S-S-E-C-Q-N-R-F-P-G-C-R-C-K-A-Q-CONH2              |
| O35  | Biotin-X-C-Q-N-R-F-P-G-C-R-C-K-A-Q-C-N-T-K-Q-C-P-CONH2              |
| P2   | Biotin-X-F-P-G-C-R-C-K-A-Q-C-N-T-K-Q-C-P-C-Y-L-A-CONH2              |
| P30  | Biotin-X-C-L-T-C-G-A-A-D-H-W-D-S-K-N-V-S-C-K-N-C-CONH2              |
| R8   | Biotin-X-F-I-S-E-Y-C-G-E-I-I-S-Q-D-E-A-D-R-R-G-K-CONH2              |
| R23  | Biotin-X-D-R-R-G-K-V-Y-D-K-Y-M-C-S-F-L-F-N-L-N-N-CONH2              |
| S4   | Biotin-X-N-N-D-F-V-V-D-A-T-R-K-G-N-K-I-R-F-A-N-H-CONH2              |
| S10  | Biotin-X-D-A-T-R-K-G-N-K-I-R-F-A-N-H-S-V-N-P-N-C-CONH2              |
| S22  | Biotin-X-N-H-S-V-N-P-N-C-Y-A-K-V-M-M-V-N-G-D-H-R-CONH2              |
| T11  | Biotin-X-R-A-I-Q-T-G-E-E-L-F-F-D-Y-R-Y-S-Q-A-D-A-CONH2              |
| ctr-D28  | Biotin-X-L-D-Q-D-G-T-F-I-E-E-L-I-K-N-Y-D-G-K-V-H-CONH2              |
| ctr-G5   | Biotin-X-I-S-S-M-F-P-D-K-G-T-A-E-E-L-K-E-K-Y-K-E-CONH2              |
| ctr-K11  | Biotin-X-D-R-E-A-G-T-E-T-G-G-E-N-N-D-K-E-E-E-E-K-CONH2              |
| TAT-peptides used in VEC-positive EC treatment |   |
| TAT-M6   | Biotin-X-N-F-C-A-I-A-R-L-I-G-T-K-T-C-R-Q-V-Y-E-F -YGRKKRRQRRR-CONH2 |
| TAT-M10  | Biotin-X-I-A-R-L-I-G-T-K-T-C-R-Q-V-Y-E-F-R-V-K-E-YGRKKRRQRRR-CONH2  |
| TAT-O4   | Biotin-X-P-C-D-H-P-R-Q-P-C-D-S-S-C-P-C-V-I-A-Q-N-YGRKKRRQRRR-CONH2  |
| TAT-P30  | Biotin-X-C-L-T-C-G-A-A-D-H-W-D-S-K-N-V-S-C-K-N-C-YGRKKRRQRRR-CONH2  |
| TAT-ctr-K11                                    | Biotin-X-D-R-E-A-G-T-E-T-G-G-E-N-N-D-K-E-E-E-E-K-YGRKKRRQRRR-CONH2  |

## SUPPLEMENTAL REFERENCES

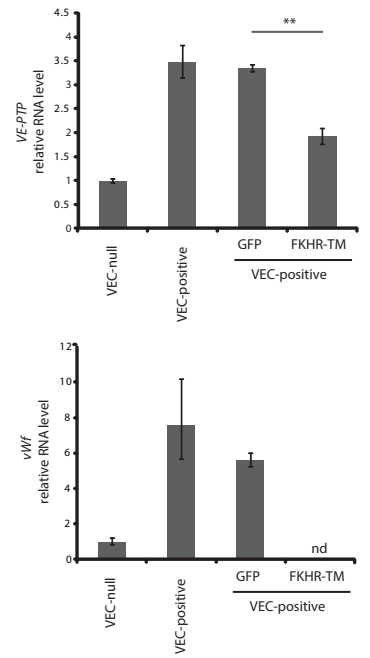
1. Balconi G, Spagnuolo R, Dejana E. Development of endothelial cell lines from embryonic stem cells: A tool for studying genetically manipulated endothelial cells in vitro. *Arteriosclerosis, thrombosis, and vascular biology*. 2000;20:1443-1451
2. Grazia Lampugnani M, Zanetti A, Corada M, Takahashi T, Balconi G, Breviario F, Orsenigo F, Cattelino A, Kemler R, Daniel TO, Dejana E. Contact inhibition of vegf-induced proliferation requires vascular endothelial cadherin, beta-catenin, and the phosphatase dep-1/cd148. *The Journal of cell biology*. 2003;161:793-804
3. Navarro P, Caveda L, Breviario F, Mandoteanu I, Lampugnani MG, Dejana E. Catenin-dependent and -independent functions of vascular endothelial cadherin. *The Journal of biological chemistry*. 1995;270:30965-30972
4. Lampugnani MG, Zanetti A, Breviario F, Balconi G, Orsenigo F, Corada M, Spagnuolo R, Betson M, Braga V, Dejana E. Ve-cadherin regulates endothelial actin activating rac and increasing membrane association of tiam. *Molecular biology of the cell*. 2002;13:1175-1189
5. Xiao K, Allison DF, Kottke MD, Summers S, Sorescu GP, Faundez V, Kowalczyk AP. Mechanisms of ve-cadherin processing and degradation in microvascular endothelial cells. *The Journal of biological chemistry*. 2003;278:19199-19208
6. Cattelino A, Liebner S, Gallini R, Zanetti A, Balconi G, Corsi A, Bianco P, Wolburg H, Moore R, Oreda B, Kemler R, Dejana E. The conditional inactivation of the beta-catenin gene in endothelial cells causes a defective vascular pattern and increased vascular fragility. *The Journal of cell biology*. 2003;162:1111-1122
7. Bussolino F, De Rossi M, Sica A, Colotta F, Wang JM, Bocchietto E, Padura IM, Bosia A, DeJana E, Mantovani A. Murine endothelioma cell lines transformed by polyoma middle t oncogene as target for and producers of cytokines. *Journal of immunology*. 1991;147:2122-2129
8. Dull T, Zufferey R, Kelly M, Mandel RJ, Nguyen M, Trono D, Naldini L. A third-generation lentivirus vector with a conditional packaging system. *Journal of virology*. 1998;72:8463-8471
9. Daly C, Wong V, Burova E, Wei Y, Zabski S, Griffiths J, Lai KM, Lin HC, Ioffe E, Yancopoulos GD, Rudge JS. Angiopoietin-1 modulates endothelial cell function and gene expression via the transcription factor foxo1. *Genes & development*. 2004;18:1060-1071
10. Quaschnicka H, Slater SC, Beeching CA, Boehm M, Sala-Newby GB, George SJ. Regulation of smooth muscle cell proliferation by beta-catenin/t-cell factor signaling involves modulation of cyclin d1 and p21 expression. *Circulation research*. 2006;99:1329-1337
11. Lampugnani MG, Corada M, Andriopoulou P, Esser S, Risau W, Dejana E. Cell confluence regulates tyrosine phosphorylation of adherens junction components in endothelial cells. *Journal of cell science*. 1997;110 ( Pt 17):2065-2077
12. Kim D, Pertea G, Trapnell C, Pimentel H, Kelley R, Salzberg SL. Tophat2: Accurate alignment of transcriptomes in the presence of insertions, deletions and gene fusions. *Genome Biol*. 2013;14:R36
13. Durinck S, Moreau Y, Kasprzyk A, Davis S, De Moor B, Brazma A, Huber W. Biomat and bioconductor: A powerful link between biological databases and microarray data analysis. *Bioinformatics*. 2005;21:3439-3440
14. Love MI, Huber W, Anders S. Moderated estimation of fold change and dispersion for rna-seq data with deseq2. *Genome Biol*. 2014;15:550
15. Huang da W, Sherman BT, Lempicki RA. Systematic and integrative analysis of large gene lists using david bioinformatics resources. *Nat Protoc*. 2009;4:44-57
16. Spagnuolo R, Corada M, Orsenigo F, Zanetta L, Deuschle U, Sandy P, Schneider C, Drake CJ, Breviario F, Dejana E. Gas1 is induced by ve-cadherin and vascular endothelial growth factor and inhibits endothelial cell apoptosis. *Blood*. 2004;103:3005-3012
17. Cartharius K, Frech K, Grote K, Klocke B, Haltmeier M, Klingenhoff A, Frisch M, Bayerlein M, Werner T. MatInspector and beyond: Promoter analysis based on transcription factor binding sites. *Bioinformatics*. 2005;21:2933-2942
18. Taddei A, Giampietro C, Conti A, Orsenigo F, Breviario F, Pirazzoli V, Potente M, Daly C, Dimmeler S, Dejana E. Endothelial adherens junctions control tight junctions by ve-cadherin-mediated upregulation of claudin-5. *Nature cell biology*. 2008;10:923-934

19. Giampietro C, Disanza A, Bravi L, Barrios-Rodiles M, Corada M, Frittoli E, Savorani C, Lampugnani MG, Boggetti B, Niessen C, Wrana JL, Scita G, Dejana E. The actin-binding protein eps8 binds ve-cadherin and modulates yap localization and signaling. *J Cell Biol.* 2015;211:1177-1192
20. Nakae J, Kitamura T, Kitamura Y, Biggs WH, 3rd, Arden KC, Accili D. The forkhead transcription factor foxo1 regulates adipocyte differentiation. *Developmental cell.* 2003;4:119-129
21. Konze KD, Ma A, Li F, Barsyte-Lovejoy D, Parton T, Macnevin CJ, Liu F, Gao C, Huang XP, Kuznetsova E, Rougie M, Jiang A, Pattenden SG, Norris JL, James LI, Roth BL, Brown PJ, Frye SV, Arrowsmith CH, Hahn KM, Wang GG, Vedadi M, Jin J. An orally bioavailable chemical probe of the lysine methyltransferases ezh2 and ezh1. *ACS chemical biology.* 2013;8:1324-1334
22. Corada M, Orsenigo F, Morini MF, Pitulescu ME, Bhat G, Nyqvist D, Breviario F, Conti V, Briot A, Iruela-Arispe ML, Adams RH, Dejana E. Sox17 is indispensable for acquisition and maintenance of arterial identity. *Nature communications.* 2013;4:2609
23. Corada M, Liao F, Lindgren M, Lampugnani MG, Breviario F, Frank R, Muller WA, Hicklin DJ, Bohlen P, Dejana E. Monoclonal antibodies directed to different regions of vascular endothelial cadherin extracellular domain affect adhesion and clustering of the protein and modulate endothelial permeability. *Blood.* 2001;97:1679-1684
24. Hayashi M, Majumdar A, Li X, Adler J, Sun Z, Vertuani S, Hellberg C, Mellberg S, Koch S, Dimberg A, Koh GY, Dejana E, Belting HG, Affolter M, Thurston G, Holmgren L, Vestweber D, Claesson-Welsh L. Ve-ptp regulates vegfr2 activity in stalk cells to establish endothelial cell polarity and lumen formation. *Nature communications.* 2013;4:1672

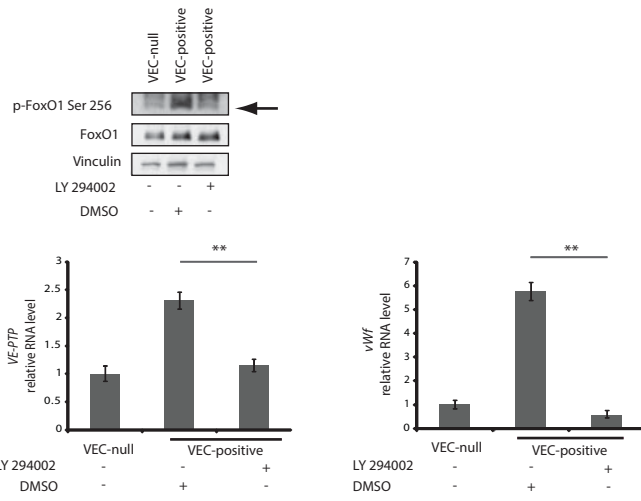
**A**



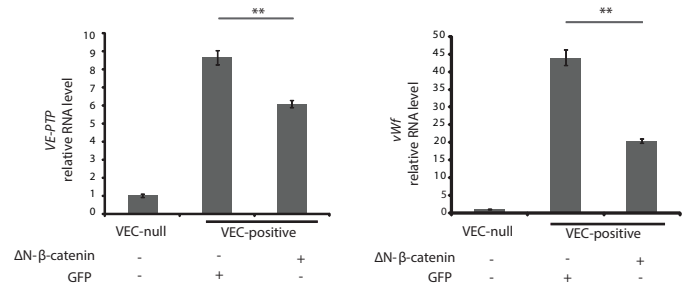
**B**



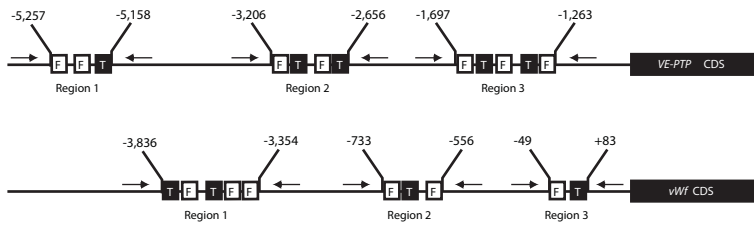
**C**



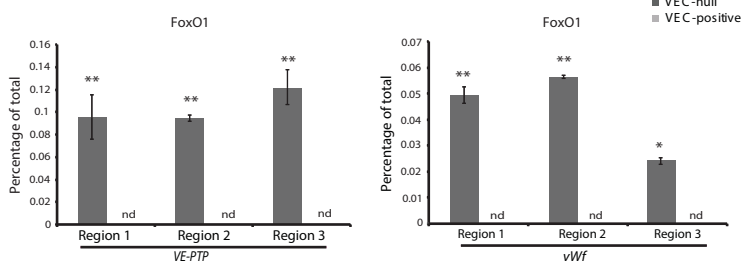
**D**



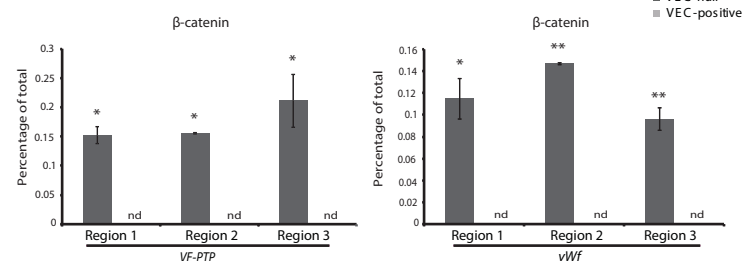
**E**

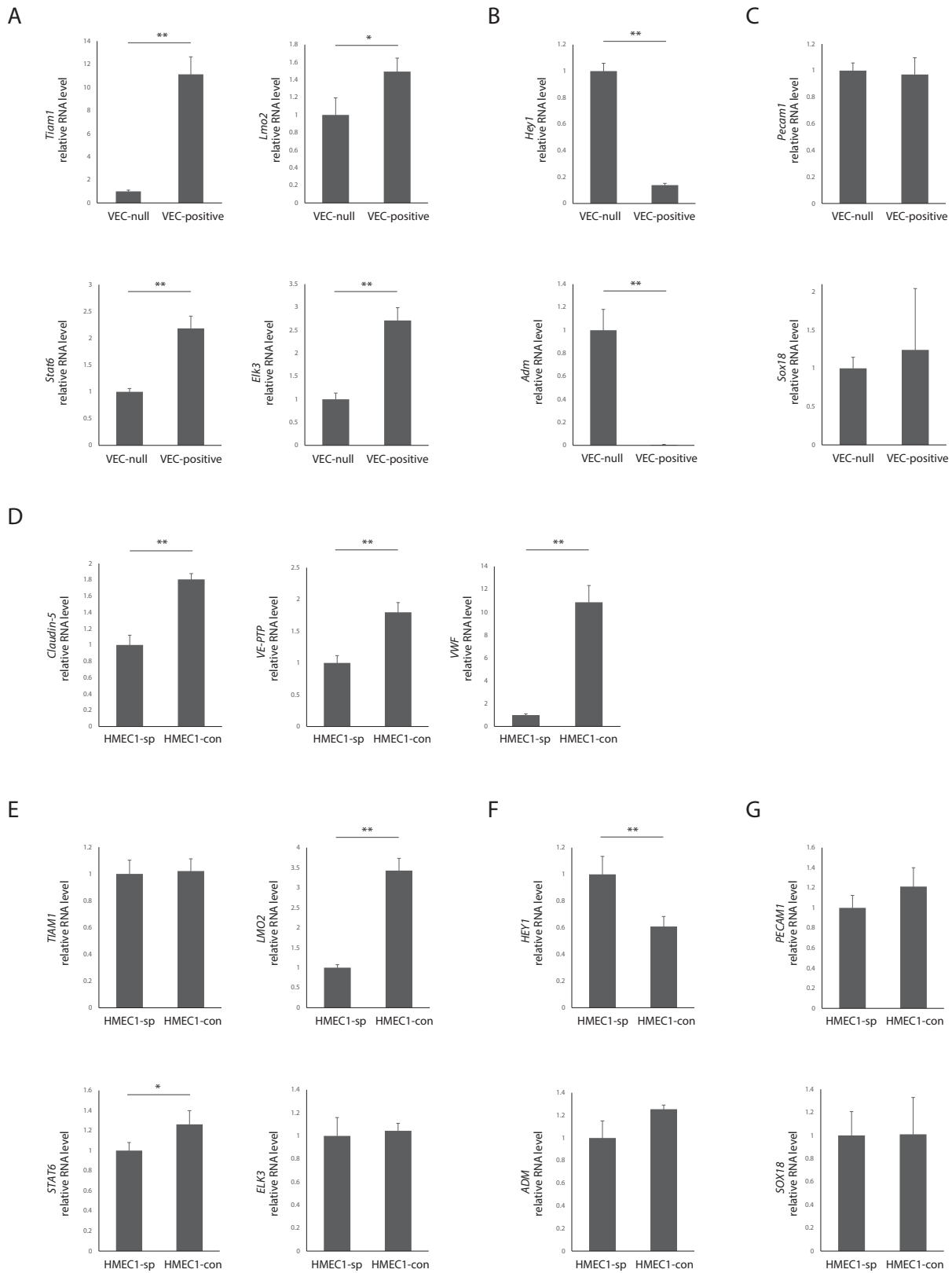


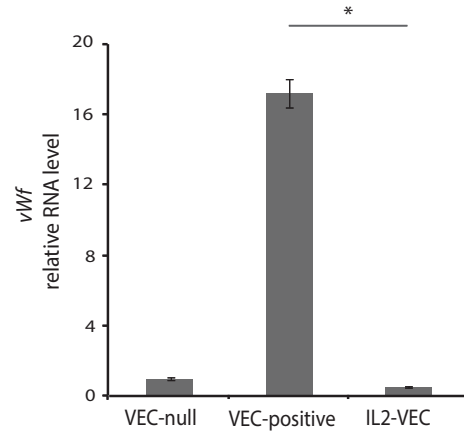
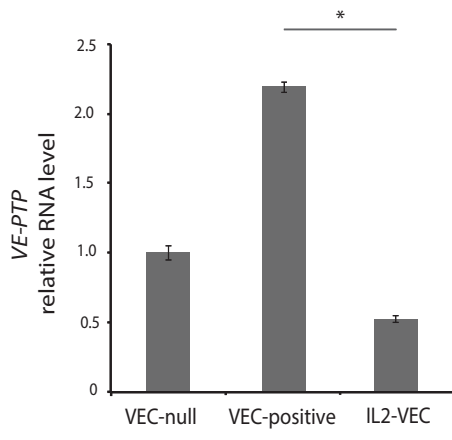
**F**



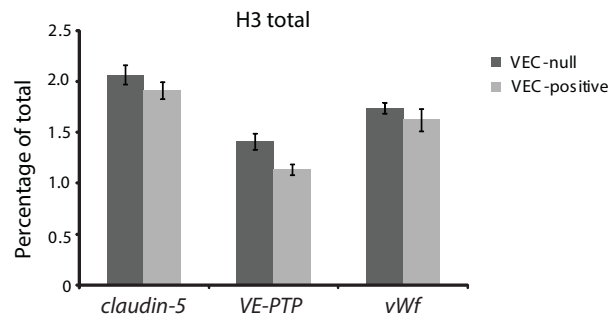
**G**





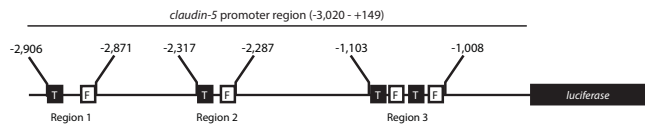


Online Figure III

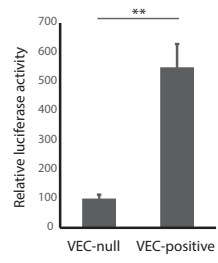


Online Figure IV

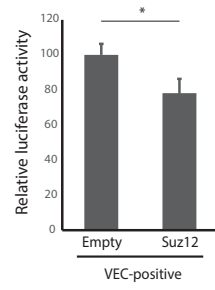
A



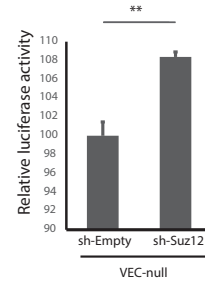
B



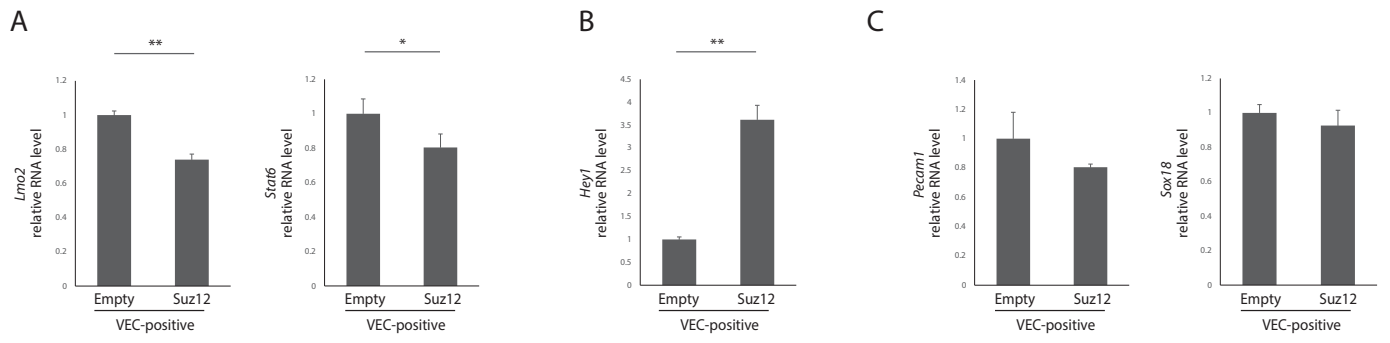
C



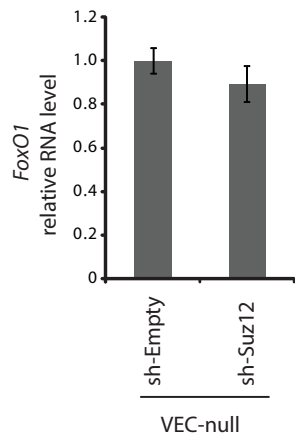
D



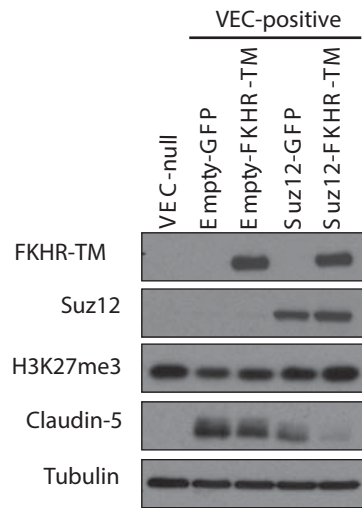
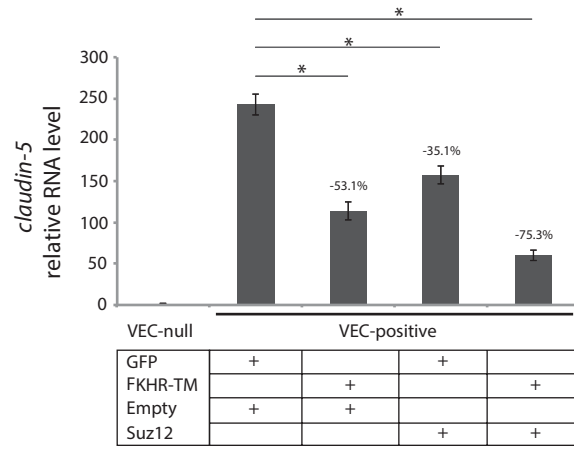
Online Figure V



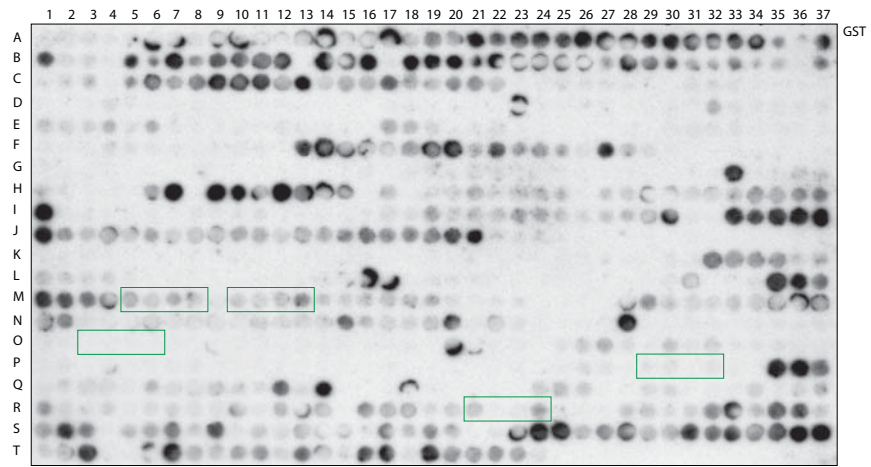
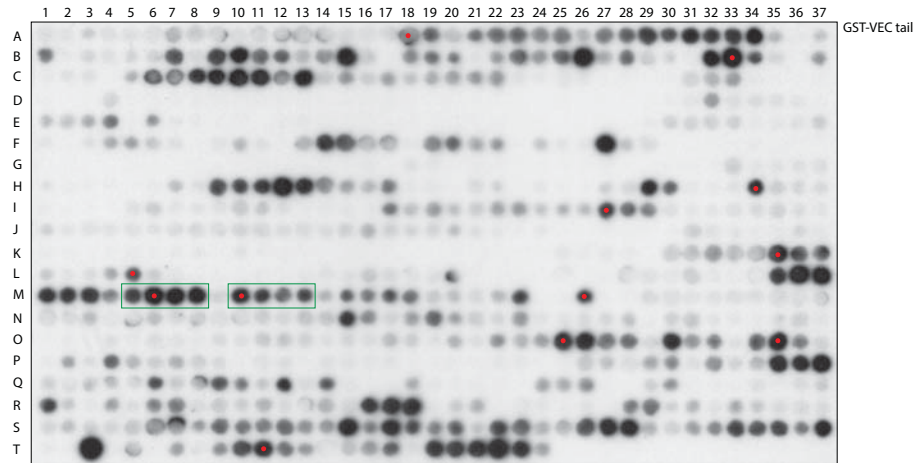
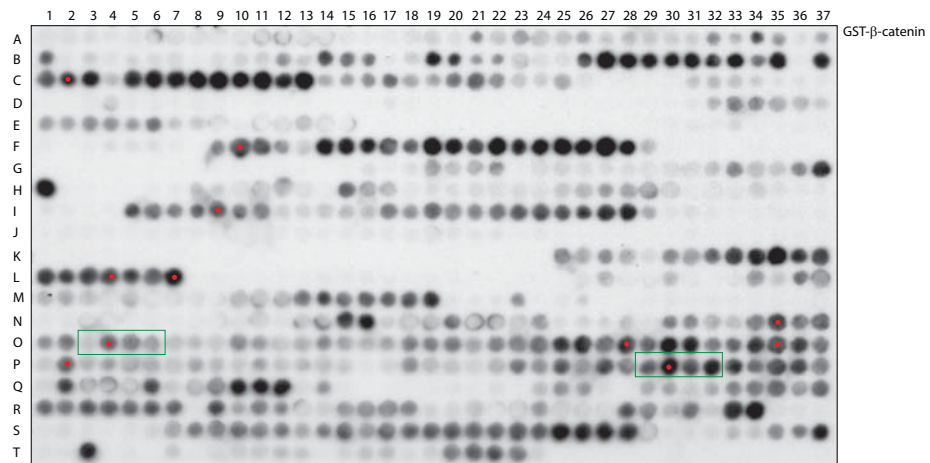
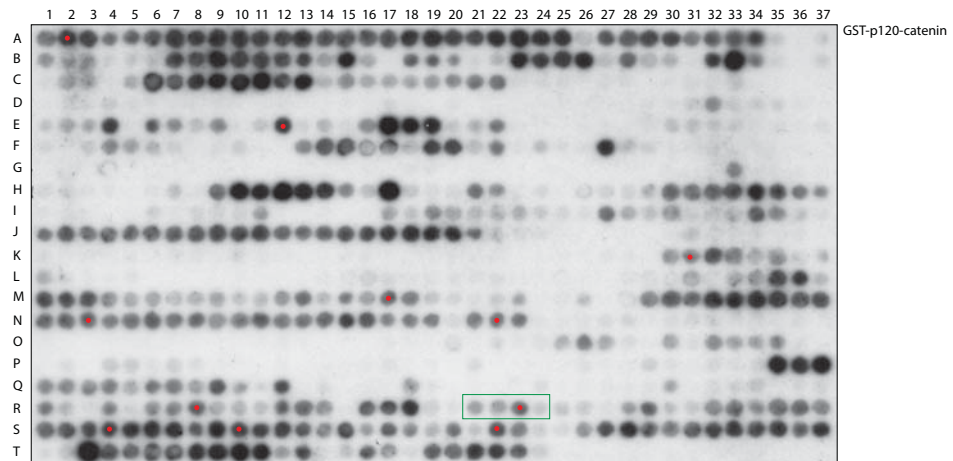
Online Figure VI

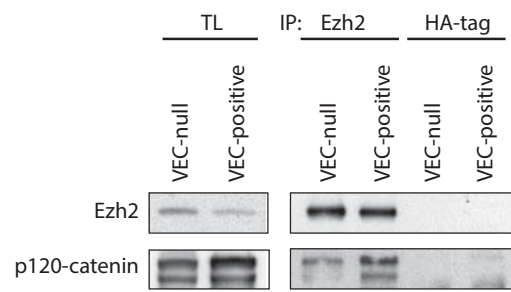


Online Figure VII

**A****B**

Online Figure VIII

**A****B****C****D**

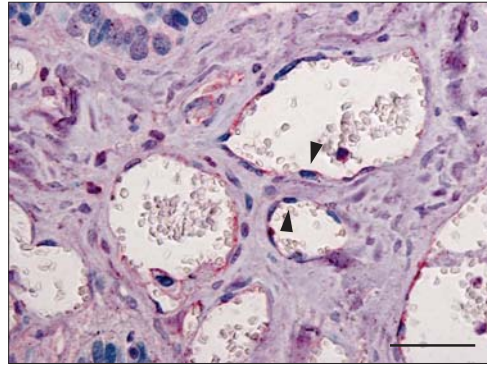
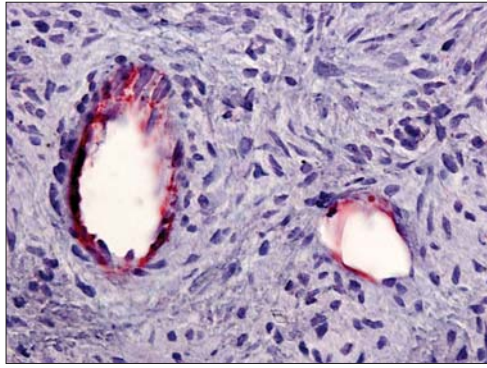


Online Figure X

Healthy ovary

Ovarian cancer

EZH2 VE-PTP



Online Figure XI